uOttawa

L'Université canadienne
Canada's university

FACULTÉ DES ÉTUDES SUPÉRIEURES ET POSTOCTORALES

uOttawa

L'Université canadienne
Canada's university

FACULTY OF GRADUATE AND POSDOCTORAL STUDIES

Raphaelle Cardyn

AUTEUR DE LA THÈSE / AUTHOR OF THESIS

M.Sc. (Earth Sciences)

GRADE / DEGREE

Department of Earth Sciences

FACULTÉ, ÉCOLE, DÉPARTEMENT / FACULTY, SCHOOL, DEPARTMENT

Analysis of gases in ice from regions of northern Canada

TITRE DE LA THÈSE / TITLE OF THESIS

I. Clark

DIRECTEUR (DIRECTRICE) DE LA THÈSE / THESIS SUPERVISOR

CO-DIRECTEUR (CO-DIRECTRICE) DE LA THÈSE / THESIS CO-SUPERVISOR

EXAMINATEURS (EXAMINATRICES) DE LA THÈSE / THESIS EXAMINERS

D. Fisher

H. French

Gary W. Slater

LE DOYEN DE LA FACULTÉ DES ÉTUDES SUPÉRIEURES ET POSTDOCTORALES /
DEAN OF THE FACULTY OF GRADUATE AND POSTDOCORAL STUDIES

Analysis of gases in ice from regions of northern Canada

by

Raphaelle Cardyn

A thesis submitted to the Faculty of Graduate and Postdoctoral Studies in partial fulfillment of the requirements for the degree of M.Sc. in Earth Sciences

Department of Earth Sciences
Faculty of Science
University of Ottawa

Your file Votre référence
ISBN: 0-494-11230-1
Our file Notre référence
ISBN: 0-494-11230-1

Abstract

Gas bubbles in ice hold relevance to the origin and process of formation, distinguishing between an atmospheric or dissolved origin. An extraction line was built to isolate gases from ice, and tested using glacial, aufeis and ground ice from the Canadian Arctic. A newly developed mass spectrometry technique was used to analyze the gases for gas ratios of three principal atmospheric gases (N_2, O_2, and Ar) as well as ^{18}O and ^{15}N of these gases. O_2/Ar and N_2/Ar ratios demonstrate differences between atmospheric gas in glacial ice and gases exsolved from freezing water, due to the difference in their relative solubilites. Glacial and ground ice contained higher oxygen-18 values than the atmosphere and aufeis ice. Results for glacier ice show that isotopic and gas ratios of atmospheric gas entrapped during glacial ice formation change through gravitational settling. Aufeis ice bubbles originate as dissolved gas with alteration by excess air addition and/or mixing with snow pack. In the ground ice sampled, low oxygen concentrations and high $\delta^{18}O$ values, indicate respiration prior to formation.

Résumé

Les gaz se trouvant dans la glace détiennent de l'information quant à l'origine et aux processus de formation. La distinction entre les gaz d'origine atmosphérique et les gaz d'origine dissoute est difficile à établir en utilisant des méthodes d'analyses traditionnelles. Une ligne d'extraction a été construite pour isoler les gaz des glaciers, de la glace de sol et de la glace d'aufeis de l'Arctique canadien. Une technique de spectrométrie de masse a été mise au point pour comparer les rapports gazeux et isotopiques des trois principaux gaz atmosphériques ((N_2, O_2 et Ar) se trouvant dans la glace. Les gaz atmosphériques dans les glaciers se distinguent des gaz exsolus lors du gel de l'eau par leurs différentes proportions de O_2/Ar et de N_2/Ar. Les glaciers et les glaces de sol avaient des valeurs plus élevées d'oxygène-18 que l'atmosphère et la glace d'aufeis. L'effet du fractionnement lors de l'occlusion des gaz dans la glace est observé dans les valeurs des rapports gazeux et isotopiques. Les gaz dans la glace d'aufeis sont d'abord dissous dans les eaux souterraines, puis affectés par l'air en excédent et/ou par un mélange avec la neige. Les faibles concentrations en oxygène associées à des valeurs élevées en $\delta^{18}O$ sont signes de respiration précédant la formation de glace de sol.

Acknowledgments

First of all I would like to thank my supervisor Dr. Ian Clark for believing I could go through with this project, for supporting me throughout and for his help with my many concerns and questions. You have showed me that isotopes are in fact not that scary.

I also have to thank Shane Greene without whom this would not have been possible. Your constant mental support and answers to my godzillion questions helped me see the light.

Fabrice Calmels, for providing me with some ground ice and some good laughs in the cutting room.

Natural Resources Canada employees, David Fisher and Chris Zdanowicz, for providing me with ice cores, James Zheng for helping me in the cutting room and Mike Demuth for bringing me on one of his glacier expeditions in British Columbia.

My parents, for the good example they showed me and for helping me financially during my studies.

I would like to thank Todd Sowers for taking the time to show me his lab and extraction technique. I could not have finished this thesis without a special mention to the G.G. Hatch isotope lab staff at the University of Ottawa who showed me that I can be in a lab without blowing the place up.

Table of contents

List of figures

List of tables

1 Introduction

1.1 Terms of reference and study objectives

With climate change and global warming currently at the center of scientific discussion increased interest has been given to the occurrence of buried ice its use in predicting subsequent impacts of warming (Dredge et *al.*, 1999; St-Onge and McMartin, 1999; Dyke and Savelle, 2000; Murton et *al.*, 2005). Reconstructions of the extent of past glaciations during the Quaternary have included detailed investigations into the origin of buried ice bodies in the Arctic (Murton et *al.*, 2005). Although they have been studied over a long period of time, the origin of some buried ice forms remain unknown. Periglacial and glacial environments host several examples of ice forms such as buried ice, ground ice, aufeis ice, buried snow banks, ice caps, and glaciers. In most cases, the origin of these ice formations is enigmatic but show great potential in expanding our knowledge on climate process in these areas.

Many approaches have been taken in order to understand more about ice. For example;

- Isotopic content and concentrations of gas trapped in ice cores have been used to identify glacial-interglacial changes (Neftel et *al.*, 1988; Chappellaz et *al.*, 1990, Barnola et *al.*, 1991) as well as variation in isotopic content in the atmosphere (Craig et *al.*, 1988, Sowers and Bender, 1989, Sowers et *al.*, 1991) and atmospheric gas concentration over time (Caillon et *al.*, 2003).
- Zheng et *al.* (1998) used electrical conductivity of ice to study volcanic acid layers in ice cores.
- Calmels and Allard (2004) used tomodensitometry to establish proportion of sediment/ice/gas content in cores to monitor thermal gradient fluctuation during the formation of mounds.

- Craig et *al.* (1988) used isotopic ratios of gas in bubbles in ice cores as evidence of gravitational settling to partly explain the difference between gas ratios and isotopes of free atmospheric gas and gases trapped in ice cores.
- Ice fabric crystals in polar ice sheets are related to compression and were modeled by Castelnau and Duval (1994) and by Morland and Staroszczyk (1998).
- Ice crystallography was used to identify layers in Antarctica (Guglielmin et *al.*, 2002).
- Major ions of high altitude, cold alpine glacial ice were studied to measure seasonal fluxes recorded in the ice (Maupetit et *al.*, 1995).

These numerous studies indicate that many factors affect ice characteristics and the concentration of gas in bubbles trapped within ice. One factor of particular importance to this research that affect gas concentration is gas solubility in water. The solubility of gases in water varies from one atmospheric gas to another and consequently ratios of dissolved gases such as O_2/Ar will be different from those same ratios in the atmosphere. Bubbles in ice produced by the freezing of water will have different gas concentrations than bubbles produced by trapping of atmospheric gas through firn densification and occlusion during glacial ice formation. With this in mind, the main objectives of this research are focused around developing a new technique to determine the origin of ice formations based on isotopic ratios and gas ratios for gases trapped in bubbles in ice.

There are 2 principal objectives involved in this research project:

1. The first objective is to set into place a method for technical analysis. This includes building a working line for the extraction of gases present in bubbles trapped in ice as well as developing the mass spectrometry techniques and corrections.
2. The second objective is to analyze different types of ice, namely aufeis, ground and glacier ice to test the method and qualitatively identify unique isotopic or gas ratios and signatures for each types of ice.

1.3 Gas entrapped in ice

In certain types of ice, gas bubbles can be found (Murton et *al.*, 2005) which may provide a tool for finding the origin of the ice and conditions of formation. The following describes the different mechanisms by which gas bubbles may be generated and preserved in ground ice, aufeis ice and glacier ice.

1.3.1 Atmospheric gas and their entrapment in glacial ice

Of the different types of ice, glacier ice is unique in that it holds information about the atmosphere at the time of accumulation of those specific layers of ice. This information can provide insight on past climate and atmospheric conditions.

The main gases found in the atmosphere are nitrogen, oxygen, argon and carbon dioxide. Table 1 displays their content by volume (Handbook of chemistry and physics, 1970).

Table 1 Atmospheric content of the four most abundant gases in air

Element	Formula	Molar fraction in atmosphere
Nitrogen	N_2	0.78084
Oxygen	O_2	0.20946
Argon	Ar	0.00934
Carbon Dioxide	CO_2	0.00033

Atmospheric gas within glacial ice goes through 4 zones before being trapped in the ice: the upper convective zone, the diffusive air column, the non-diffusive zone and the bubble close-off region (Sowers and Bender, 1992; Schwander, 1996).

The upper convective zone is located at the top of the firn on the glacier and gas composition is the same as the atmosphere above. Movement of the gas in this zone is mainly achieved by surface winds through advection and atmospheric pressure fluctuations. Deeper in the firn, the porosity of vacant air space decreases which reduces airflow from the surface until it is negligible compared to molecular diffusion.

This is where the diffusive air column is located. Within this zone, gas moves strictly by molecular diffusion. Gravitational settling here causes enrichment of heavy isotopes with depth, which in turn slightly alters the chemical and isotopic composition of the gas from the atmospheric values.

Below the diffusive air column is the non-diffusive zone in which diffusivity is so low that the gases can not reach diffusive equilibrium before they are occluded into a bubble. This zone is not always present in which cases air moves directly from the diffusive air column to the bubble close-off region.

This is the zone where air is finally occluded in the ice and is located at the bottom of the firn where ice density is between 0.795 g/cm^3 and 0.830 g/cm^3 (Craig et *al.*, 1988; Sowers and Bender, 1992).

Depending on location, elevation, temperature and accumulation rates, the process of occluding air in ice can take anywhere between several years to thousands of years. For this reason, the age of the gas is younger than the age of the ice (Barnola et *al.*, 1991).

Isotopic values from previous studies on Greenland and Antarctic ice show that fractionation may occur during accumulation of firn and therefore might affect isotopic composition of gases in the ice cores. The main fractionation process is gravitational settling which acts as a columnar sieve for isotopes. During settling, gases located deeper in the firn become enriched in heavy isotopes such as ^{15}N and ^{18}O and in heavy gases (Craig et *al.*, 1988, Caillon et *al.*, 2003). Enrichment of heavy gases alters gas composition and consequently gas ratios will change. For example, O_2/N_2, Ar/O_2 will increase.

The isotopic content of air found in glacial ice is also affected by the initial atmospheric content which may vary over time. The isotopic content of oxygen in the atmosphere is determined by a number of factors. For example;

- Precipitation (Dansgaard, 1964), seawater and biological isotopic effects (Bender et *al.*, 1985) such as respiration. During respiration, the lighter isotopes of oxygen are preferentially consumed by organisms (Schleser, 1979; Quay and al., 1995). Therefore, $\delta^{18}O$ of atmospheric O_2 tends to be higher than that of seawater, with an average value of +23.5 ‰ SMOW (Kroopnick and Craig, 1972).

- Amount of evapotranspiration from the surface of leaves (Dongman, 1974; Sowers and Bender, 1989).

The isotopic content of N_2 in atmosphere, ^{15}N, is constant on a global scale and has a residence time greater than 10 millions years (Hattori, 1983; Mariotti, 1983). Argon, an inert element, is also very constant with respect to the biogeochemical cycle (Sowers and Bender, 1989) and content changes little over time. In addition, a change in the last century is also observed in the O_2/Ar measurements due to the consumption in fossil fuel combustion as well as land use (Sowers et *al.*, 1997). Table 2 displays the oxygen and nitrogen molar gas ratio to argon as found in the atmosphere today.

Table 2 Atmospheric gas molar ratios

Gas ratio	Molar ratio
O_2/Ar	22.43
N_2/Ar	83.60

Air trapped in glacier ice essentially represents the atmosphere at time of bubble close-off. Aside from gravitational and isotopic fractionation, values should be close to atmospheric values. If variations are observed in the glacial record, they are most likely a result of one or a combination of the following reasons:

- adjacent bubbles may have been closed at a slightly different depth creating different fractionation conditions;
- micro-fractures may have enabled air to escape while the ice was relaxing after coring or;
- chemical reaction within the ice affected the gas composition (Sowers and Bender, 1989).

The rate at which gases can be lost through micro-fractures is dependent on the molecular diameter of those gases (Craig et *al.*, 1988). Since Ar has a smaller diameter than O_2, and O_2 has a smaller diameter than N_2, Ar will diffuse faster than O_2, which will in turn diffuse faster than N_2. Because of their respective diffusivity, the gas ratios, O_2/Ar and N_2/Ar, will be increased.

Isotopic content in gas entrapped in glacial ice has values ranging between 0 ‰ and 0.8 ‰ for $\delta^{18}O$ (Sowers and Bender, 1989; Caillon et *al.*, 2003) and 0.05 ‰ to 0.5 ‰ for $\delta^{15}N$ (Sowers and Bender, 1989, 1992) with respect to present day atmosphere.

The isotopic ratios of gases found in bubbles trapped in glacier ice can be corrected for the gravitational fractionation effect based on the relationship between the partial pressure at the top of the diffusive column and the partial pressure at the time of bubble close off for a given gas. Because the $\delta^{15}N$ of the atmosphere is constant over time, its isotopic values are used to correct the isotopic ratios of other gases. The following barometric equation describes that partial pressure relationship (Sowers and Bender, 1992):

Equation 1

$$\frac{P_z}{P_o} = \exp\left(\frac{mgz}{RT}\right)$$

Where

P_z = partial pressure of the gas at depth (z) of bubble close off

P_o = partial pressure of the gas at the surface of the glacier

m = mass of one mole of gas (kg/mol)

g = acceleration due to gravity (9.80 m/s^2)

z = depth of bubble close off (m)

R = gas constant (8.314 J/mol K)

T = temperature (Kelvin)

For example, the $\delta^{18}O$ corrected for gravitational fractionation in gases from ice cores of GISP2 can be calculated with the following formula (Bender et *al.*, 1994):

Equation 2

$$\delta^{18}O_{atmosphere} = \delta^{18}O_{measured} - 2(\delta^{15}N_{measured})$$

During glacial to interglacial changes, isotopic values of $\delta^{18}O$ increased by approximately 1.25 ‰ in Greenland and Antarctica (Bender et *al.*, 1994). Figure 1 shows the variation of $\delta^{18}O$ of O_2 trapped in gas bubbles in Vostok (Antarctica) ice cores. The higher values of $\delta^{18}O$ are associated with colder glacial periods.

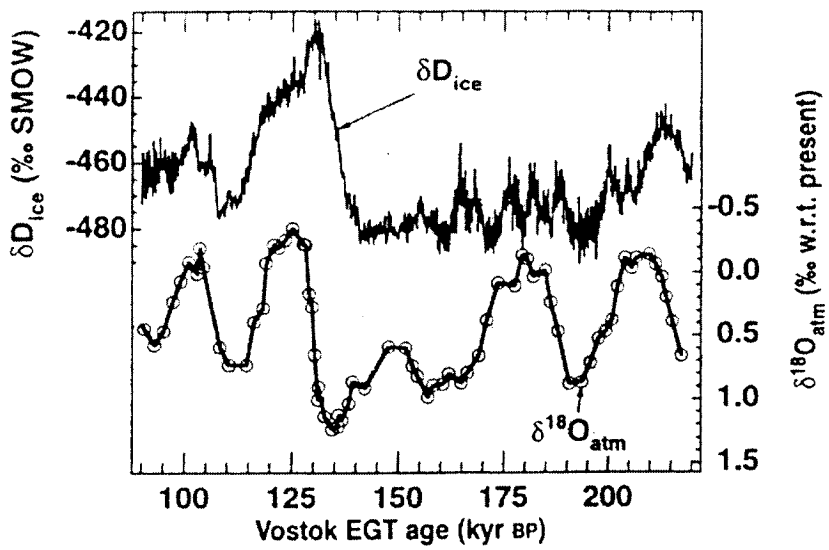

Figure 1 Isotopic ratios of $\delta^{18}O$ of O2 and δD of ice in Vostok ice cores (modified from Bender et *al.*, (1994))

Based on the same principals, gas ratios are found to be enriched in heavy gas. The following corrections can be applied to obtain the atmospheric ratios before the gravitational enrichment (Sowers and Bender, 1989):

Equation 3

$$\delta O_2 / Ar_{atmoshpere} = \delta O_2 / Ar_{measured} + 8(\delta^{15}N)$$

and

Equation 4

$$\delta N_2 / Ar_{atmosphere} = \delta N_2 / Ar_{measured} + 12(\delta^{15}N)$$

where the coefficient 8 represents the mass difference between O_2 (32) and Ar (40) and the coefficient 12 represent the mass difference between N_2 (28) and Ar (40).

1.3.2 Gases trapped in ice by freezing of water

The initial concentration of gases within the water is controlled by their respective solubility. As indicated by Henry's law (equation 1), the solubility of a gas is principally controlled by temperature and partial pressure of the gas. Henry's law mathematically describes solubility using the following equation:

Equation 5

$$K_{H_{gas}} = \frac{m_{gas}}{P_{gas}}$$

where:

K_H = Henry's constant

m = moles of gas per kg of water

P = partial pressure of the gas (mol/kg/atm).

In freshwater, the activity coefficients of the gases are equal to 1 because they are not ionized. To measure the solubility of a gas, the Henry's law constant is used:

The concentrations of gas can also be expressed as a volume, namely cc_{gas}/cc_{water} at standard temperature and pressure conditions (STP). In STP conditions, the volume occupied by 1 mole of gas is 22.414L. When expressing gases solubility as volumes and not as mole fraction, the solubility constant is called the Bunsen coefficient. The Bunsen coefficient is essentially the Henry's law constant multiplied by the gas constant (R) and site temperature (T).

Table 3 Solubility coefficients for atmospheric gases in freshwater at 0°C

Gas	Bunsen coefficient (cc/L/atm)	Henry's constant (atm/kg)
O_2	48.90	0.0215
N_2	2.37	0.0010
Ar	53.50	0.0236

Figure 2 displays how the freshwater solubility of O_2, N_2 and Ar at atmospheric equilibrium varies depending on temperature. A pressure of 1 atmosphere is assumed in calculations (Benson and Krause, 1980, 1984; CRC handbook of chemistry and physics, 1988; Andrews, 1992). As temperature increases, the solubility of gases decreases. In freshwater at atmospheric equilibrium, N_2 is more soluble than O_2 which in turn is more soluble than Ar. Consequently, the different solubility of each of these 3 gases provides an important characteristic tool. This is the ratio of each gas to the others. As seen in Figure 3, the ratio of N_2/Ar is higher and increases with temperature while O_2/Ar is lower and decreases with an increase in temperature.

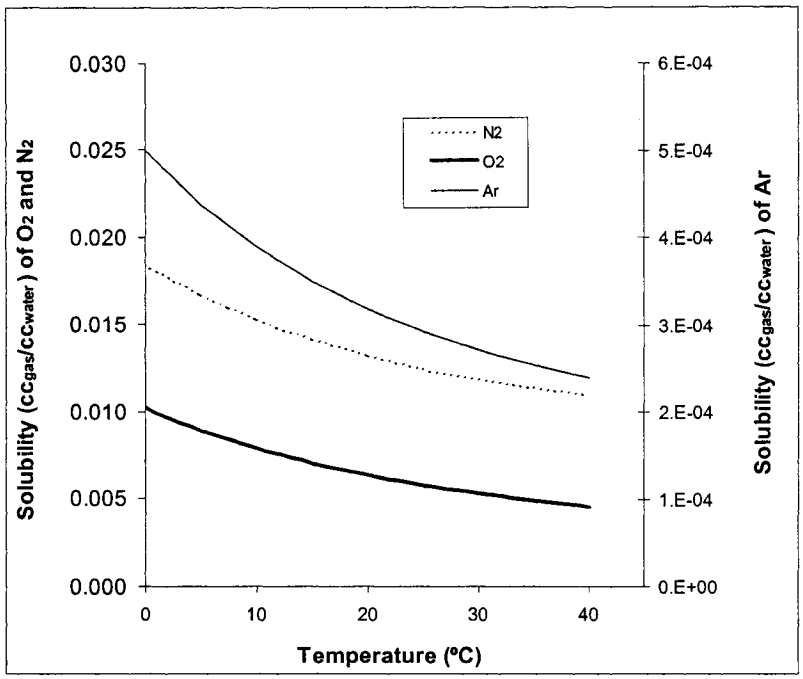

Figure 2 Freshwater solubility of O_2, N_2 and Ar at atmospheric equilibrium. The x-axis represents the temperature between 0°C and 40°C. The left y-axis shows values for the solubility in cc_{gas}/cc_{water} of O_2 and N_2 while the right y-axis shows values for the solubility in cc_{gas}/cc_{water} of Ar.

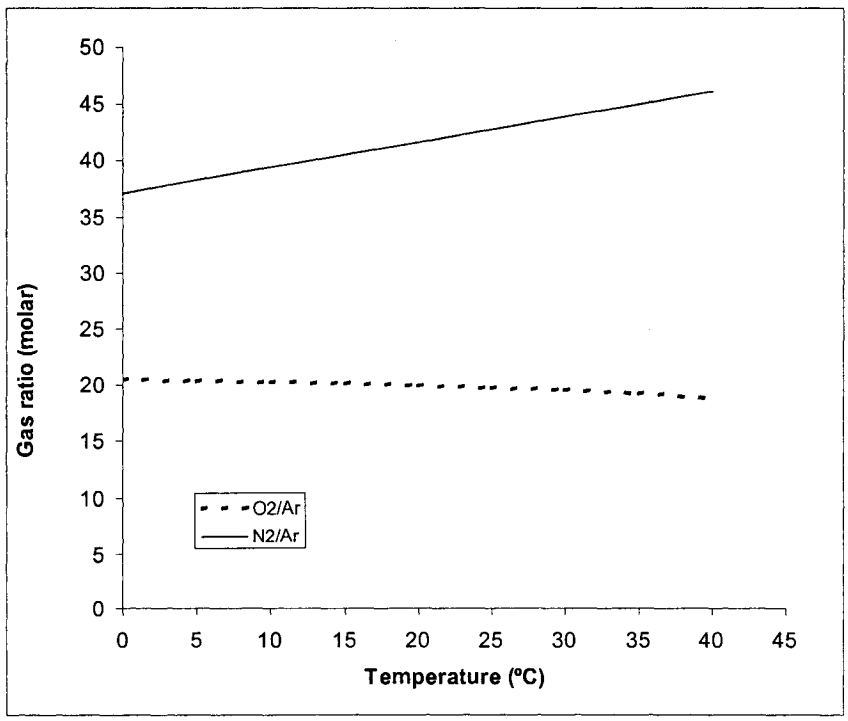

Figure 3 Dissolved O_2/Ar and N_2/Ar as a function of temperature at atmospheric equilibrium. The x-axis represents the temperature between 0°C and 40°C. The y-axis displays the molar gas ratios of O_2/Ar and N_2/Ar.

Following dissolution from the atmosphere, dissolved gas concentrations, ratios and isotopic values can be affected by several other processes including denitrification (N_2), respiration (O_2), photosynthesis, radiogenic decay (^{40}Ar) and the introduction of excess air.

Denitrification is a process in which NO_3^- is attenuated producing, amongst others products, N2 (Clark and Fritz, 1997) as described by the following equation:

$$NO_3^- + 5/4\,CH_2O \rightarrow 1/2\,N_2 + 5/4\,HCO_3^- + 1/4\,H^+ + 1/2\,H_2O$$

During the denitrification process lighter isotopes of nitrogen in NO_3^- are preferentially consumed. The result is an enriched $\delta^{15}N$ signature for the nitrate (Llund et *al.*, 2000). Conversely, it can be anticipated that the resulting N_2 of the reaction will have a depleted $\delta^{15}N$ value.

Respiration and photosynthesis can be responsible for changes in isotopic content of oxygen. Photosynthesis contributes O_2 to water while respiration consumes O_2, reducing its concentration and producing CO_2. These reactions are defined by the following simplified equation:

$$CO_2 + H_2O \underset{\textbf{respiration}}{\overset{\textbf{photosynthesis}}{\rightleftharpoons}} O_2 + CH_2O$$

During respiration, lighter isotopes of oxygen (^{16}O) are preferentially consumed over ^{18}O. When comparing photosynthesis and respiration processes, one can compare the isotopic ratios, and the gas content. If respiration prevails, $\delta^{18}O$ of dissolved oxygen in water will tend to be more enriched but the concentration will be undersaturated (Quay et *al.*, 1995).

The dissolved gases content in groundwater depends on partial pressure in the atmosphere as well as on the equilibrium temperature during gas-water exchange. The equilibrium temperature is the mean annual surface air temperature or the recharge temperature.

During recharge, it is sometimes possible to add "excess air". As water recharges to the water table from the unsaturated zone, small bubbles of air may become trapped in capillary fringe and forced down below the water table. At a certain hydrostatic pressure or (depth below the water table), those bubbles will dissolve into the water. There are three main factors influencing the excess air content in ground water: the physical aspect of the unsaturated zone and the mechanism of rain fall and recharge. If the aquifer is composed of narrow capillary fringe and small pores, it will favor the addition of excess air, for example in fine grain sediment. The pattern of rainfall and recharge may also affect the excess air component, for example, if precipitation is sporadic and sometimes heavy, the water table will rise rapidly, favoring entrapment of excess air (Heaton and Vogel, 1981).

As argon is an inert gas, its dissolved concentration will not change as a result of chemical reactions or biological activity. However, dissolved concentration can be modified by diffusion or production of argon by radiogenic decay of ^{40}K (Heaton and Vogel, 1981) which can be released from minerals in solution (Wilson and McNeill, 1997).

Fractionation can also take place as gases dissolve into water. For example, there is a +0.7‰ enrichment of oxygen-18 during dissolution of O_2 into water (Benson and Krause, 1984).

Figure 4 displays the effect of excess air on the gas ratio at a temperature of 0°C. As the excess air increases, the gas ratios evolve from those generated by atmospheric equilibrium with water towards those of the atmosphere, following an exponential curve.

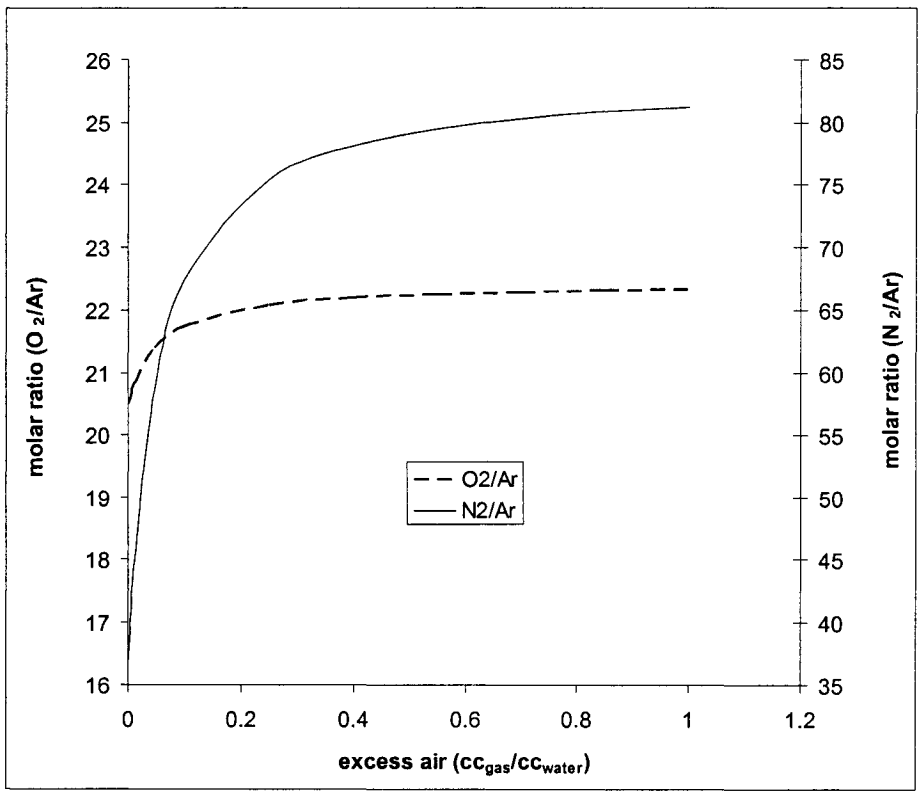

Figure 4 The effect on O_2/Ar and N_2/Ar ratio of excess air on dissolved atmospheric gas at equilibrium with atmospheric pressure

Figure 5 presents the linear relation between O_2/Ar and N_2/Ar dissolved in water at STP and the ratios found in air. As the excess air reaches 1, the ratios approach atmospheric ratios. When looking at ratios from dissolved gas in groundwater and comparing to this line, it is possible to determine if there is excess air, assuming no other process such as those described earlier have affected the gas content.

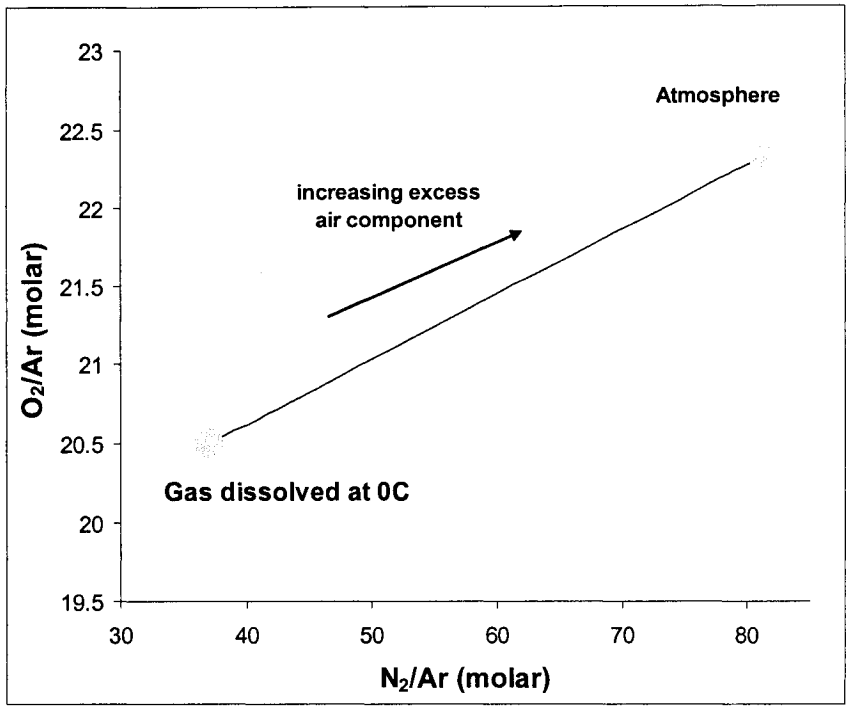

Figure 5 Relation between gases dissolved in water in equilibrium with the atmosphere and in atmosphere

Theoretically, as water found in a closed system freezes, with no solute incorporated that might influence the gas content, the concentrations of gas dissolved in the water will increases and eventually, air bubbles will nucleate in the water once it exceeds the saturation point for ambient pressure. Also, because Argon diffuses faster than nitrogen and oxygen, the ratio O_2/Ar will be enriched in air dissolved in water compared to gas in bubbles found in ice (Killawee et *al.*, 1998).

1.3.3 Formation of Aufeis ice

Aufeis ice, also know as groundwater icing or river icing, is an accumulation of overflowing water through fractures in the ice during winter months. They cover a larger area and are of greater thickness than common river over-freezing ice. There are 3 main water sources that can create aufeis ice: groundwater seepage (ground icings), perennial springs (spring icings) and stream discharge (river icings).

Ground icings are formed by suprapermafrost groundwater seeping and therefore can form anywhere, regardless of surface slope. Ground icings can also form, along with spring icings, in rivers where seasonal frost allows a river to freeze to its bottom which effectively blocks discharge along the channel. However, the buildup of hydrostatic pressure beneath the river from groundwater and/or springs can crack the overlying ice and force water discharge out of the bed and over the ice. Horizontal layers of ice accumulate over one another as the winter progresses. Spring and ground icings usually contain thin layers of ice (< 1m thick), but occasionally thicker layers (> 1m) occur as a result of increased discharge (French, 1996). The thickest layers are generally found close to the water outlet (Hu and Pollard, 1997). On average, ground icing layers are less than 1m thick and cover areas less than 0.5km2. If the river flow is low, aufeis may last throughout summer periods producing multi-annual icings (Williams and Smith, 1989; French 1996).

River icings on the other hand, form within the channel section of the river as water that has flooded upstream flows over the top of the icing. River icings have smaller gradients and thicker layers. The growth of these icings is mainly controlled by thermodynamics and hydrodynamics (Hu and Pollard, 1997). Such formations can be found in the subarctic region of Alaska and northern Canada and cause major problems in highway maintenance and construction (French 1996).

When the overflowing water freezes from both the bottom and top, exsolving gas becomes trapped by a freezing front from both direction creating bubbles trapped in the aufeis ice. The potential for direct entrapment of air (excess air) exists if discharge through ice occurs over a snow-covered surface.

1.3.4 Ice segregation, aggrading permafrost in sediments and buried glacier ice

Ground ice or intrasedimentary ice can be found in permafrost that has aggraded through saturated sediments. Aggradation of permafrost, or an increase in its extent, occurs when there is a decrease in mean ground temperature. It can be due to microclimatic changes, a variation in the ground surface conditions, or climatic changes, namely a change in the atmospheric climate (Williams and Smith, 1989).

These ice lenses and beds of ice form through the *in situ* freezing of water or by the migration of groundwater towards the freezing front during permafrost growth. At temperatures below 0°C, a cryosuction effect is developed at the freezing front due to porous structure and the surface area of particles. This suction allows movement of water for further freezing. Cryosuction is defined by the following equation:

Equation 6

$$P_i - P_w = \text{soil constant}^* (2\theta / r)$$

where

P_i = pressure of ice

P_w = pressure of water

And soil constant is a function of

θ = surface tension and soil particle volume

r = radius of curvature of the soil particle's surface (French, 1996).

Cryosuction controls the amount of water available for the freezing plane and therefore determines if segregated or pore ice will be form. For example, if the surface tension is low, a tongue of ice will move downward in the soil and slowly the pore water will freeze, forming pore ice. If there is a higher surface tension, the freezing plane will be able to grow and form thin sections of ice of a few mm to layers thicker than 1.5m. This process is called ice segregation. It usually takes place in fine-grained sediments during seasonal freezing but can also happen in permafrost zones with coarse-grained material over long periods of time. If no recrystalization occurs, elongated bubbles may form perpendicular to the ice layer. Further more, sediments may precipitate along the walls of the ice bubbles during freezing of water (Killawee et *al.*, 1998).

Throughout permafrost region in western Canadian Arctic and northern Siberia, massive ground ice and icy sediments bodies have been identified. Massive ground ice is defined as tabular ice bodies with ice content exceeding 95% in volume while icy sediments are sediments with volumetric excess ice content between 50% and 95%. Massive ground ice can occur in the form of massive segregated-intrusive ice or as buried glacier ice. Massive segregated-intrusive ice forms during glacial retreat. Subglacial meltwater travels towards the margin of the glacier due to hydraulic gradient. As the ice sheet becomes thin and retreats and there is downward permafrost aggradation, the meltwater freezes and creates massive ice bodies (Rampton, 1974, 1988, French and Harry, 1990). Buried glacier ice forms in continuous permafrost regions when till acts as an insulating cover for glaciers as they retreat. When the thickness of the till is thicker than active layer, the buried glacier ice will not melt (Lacelle et *al.*, 2004).

Traditionally, massive ice bodies in the Canadian Arctic have been identified as segregated-intrusive ice (MacKay, 1966, 1971; Dallimore and Wolfe, 1988; Harry et *al.*, 1988; Pollard and Dallimore, 1988; Pollard, 1991; MacKay and Dallimore, 1992; Lacelle et *al.*, 2004) however some scientists have begun to interpret the massive ice bodies as buried glacier ice (French and Harry, 1990; St-Onge and MacMartin, 1995; Fujino et *al.*, 1998; Dyke and Savelle, 2000). Differentiating between the two helps reconstruct the glacial and permafrost history of a location. However both types of ice have a very similar appearance in the field, detailed physical and chemical analysis must be performed to identify them.

In the Canadian Arctic, massive segregated-intrusive ice has been identified at Peninsula Point in the Northwest Territories (NWT), ~ 5km west of Tuktoyaktuk. It has been identified as refrozen meltwater from the Laurentide Ice Sheet based on the oxygen-18 content (Mac Kay and Dallimore, 1992; Moorman et *al.*, 1998). Other identified occurrences of segregated ice in the Canadian Arctic include Sabine Point on the Yukon Coastal Plain, NWT (Harry et *al.*, 1988), Lousy Point in the Richards Island, NWT (Dallimore and Wolfe, 1988), an area close to Eureka in Ellesmere Island, Nunavut (NU) (Pollard, 1991) and Nanisivik mine in northern Baffin Island, NU (Ford, 1996).

Similarly, buried glacier ice has been identified on Victoria Island near Loch Point, NWT (Lorrain and Demeur, 1985), in the Sandhills moraine on Banks Island, NWT (Harry et *al.*, 1988; French and Harry, 1990), in glaciofluvial sediments on Richards Islands, NWT (Dallimore and Wolfe, 1988), an area near Bluenose Lake, NU (St-Onge and MacMartin, 1995) and on the Wollaston Peninsula in Victoria Island, NWT (Dyke and Savelle, 2000).

Attempts have already been made to understand more about ground ice based on the gas content. For example, Brouchkov and Fukuda (2002) measured the concentration of methane in air bubbles in ice wedges and frozen soil from Siberia. It was found that methane content in air bubbles in ice wedges was lower than that in frozen soil and that older permafrost displayed higher values of methane than young permafrost. Moorman et *al.*, (1996) measured the ^{14}C content of CO_2 in air bubbles of ice bodies to date massive ground ice bodies from the Canadian north. The age obtained from the ^{14}C was younger than what was previously speculated.

1.4 Gas Extraction from Ice principles & techniques

To select an appropriate gas extraction technique and build the extraction line, a review of available techniques was completed. There are 3 main techniques for extracting gases trapped in ice: wet extraction, dry extraction and sublimation (Sowers et *al.*, 1997).

Wet extraction involves putting a sample of ice in a vessel, evacuating the vessel of all gases and then melting the ice. As the ice melts, the gas trapped in the bubbles is released. The ice is then frozen from bottom to top, forcing dissolved gas out of the ice. Dry extraction requires a stainless steel vessel in which the ice sample is introduced, followed by mechanical crushing or grating of the ice to release the air. The sublimation technique requires a glass vessel to hold the ice. Using infrared light, the ice is heated to just below the melting point under vacuum condition. Eventually, water vapor and trapped gas are cryogenically removed using cold traps.

Each technique provides a different level of efficiency in extracting gases. The wet extraction and sublimation technique allow the release of all gas trapped in bubbles, as well as air dissolved in the ice. Wet extraction is particularly useful for studies of gases that are relatively insoluble and chemically stable in water such as O_2, Ar, N_2 and CH_4. Generally, the efficiency is above 99%. The dry extraction doesn't allow liberation of all the gases from the bubbles and likely not from the dissolved gases in the ice either. This technique is useful when the goal is to obtain information about gases, such as CO_2, that are highly soluble in water. Generally, the efficiency is below 80% (Sowers et *al.*, 1997).

2 Sampling location and description

Sites throughout northern Canada have been selected in order an attempt sample ice containing two different types of gas bubbles: occluded atmospheric gas and exsolved gas trapped in bubbles in ice. Ice containing atmospheric gas was sampled from 2 glaciers located on Ellesmere Island (Agassiz Ice Cap) and Baffin Island (Barnes Ice Cap). Aufeis and ground ice sampled from northern Yukon and northern Quebec, respectively, provided the opportunity to look at exsolved gas trapped in ice (Figure 6). A general description of each site can be found in the following section.

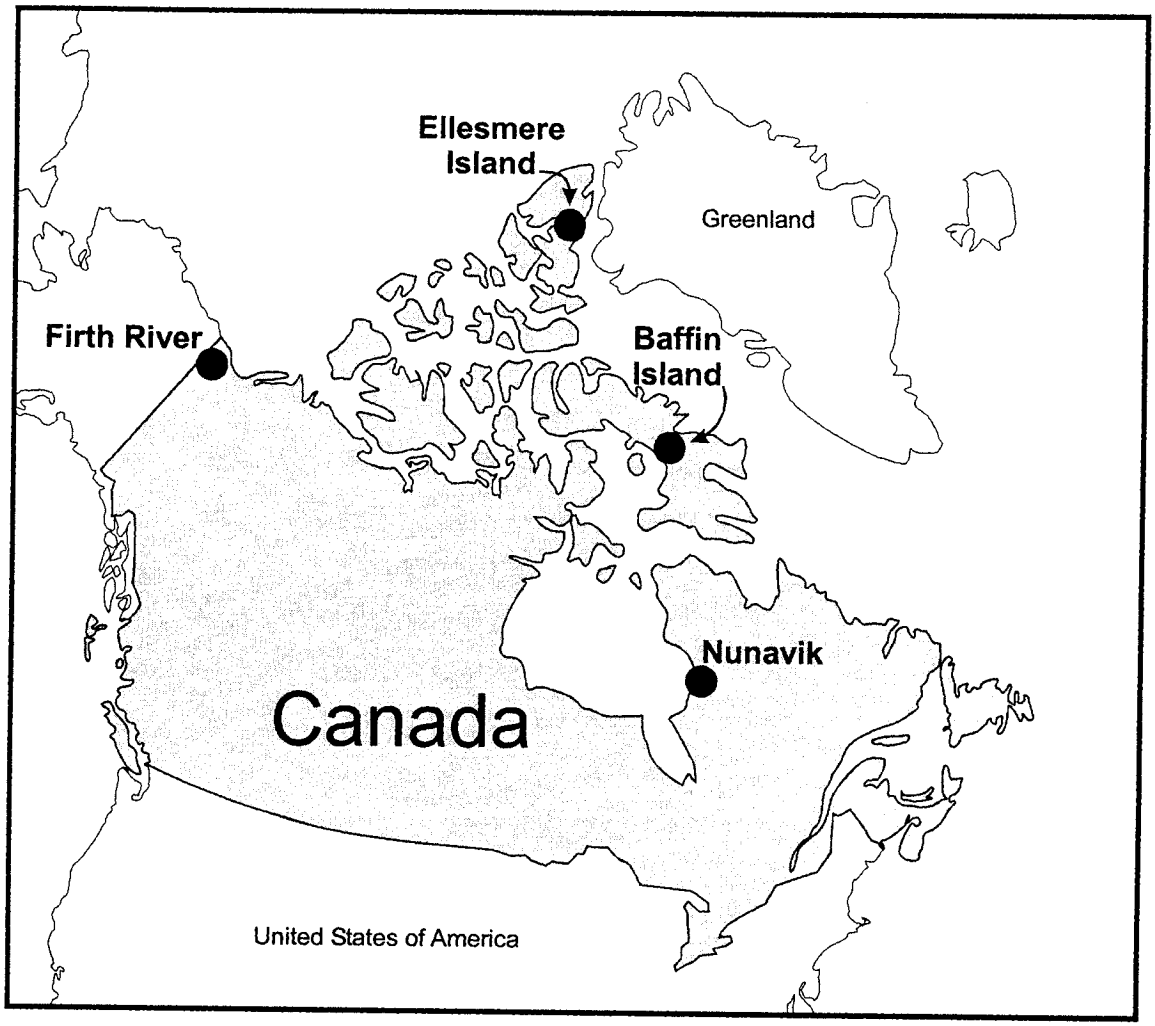

Figure 6 Sample site location map

2.1 Agassiz Ice Cap

Ellesmere Island is home to the Agassiz ice cap which covers an area of roughly 16,000 km^2. It is located in northern Canada, between latitudes 79°45' and 81°N (Figure 8). Agassiz ice cap is on the northern part of the island (Fisher et *al.*, 1983) at an elevation of 1,730m a.s.l.

Glaciers covering the area during the Wisconsinian started to retreat during the early to mid-Holocene. Melt records of the Agassiz Ice cap show that between 3,000 and 100 years before present (BP) the glacier had a persistent positive balance suggesting an advance of the glacier (Koerner and Fisher, 1990). The oldest layers of Agassiz were dated to 11,000 yr BP (Fisher et *al.*, 1983).

In ice equivalent, it receives 0.098m yr^{-1} of annual precipitation and on average 5.1% of this melts during the summer but re-freezes again in the same year (Zheng et *al.*, 1998). Agassiz has an undulating surface and several glaciers flowing between surrounding mountains drain the ice cap. The glacier lies mainly on early proterozoic granitic gneiss.

Drilling of the ice cores was completed in 1993 by personnel from the Geological Survey of Canada (GSC), using an electromechanical drill. Ice analyzed in this research project is from cores A93.1 and A93.2 (Figure 7) taken 2m apart in the same drilling pit. Dimensions of the resulting cores are a length of 1m and a diameter of 8.4cm. Ambient air temperature during coring was approximately –18 °C. Ice was stored in plastic lay-flat tubes inside core boxes and were cooled at –45°C several days before shipping. Full cores for A93.2 and half-cores for A93.1 were shipped to Ottawa. Once in Ottawa, they were then kept in a -10°C walk-in freezer. For further information, consult Zheng et *al.*, 1998.

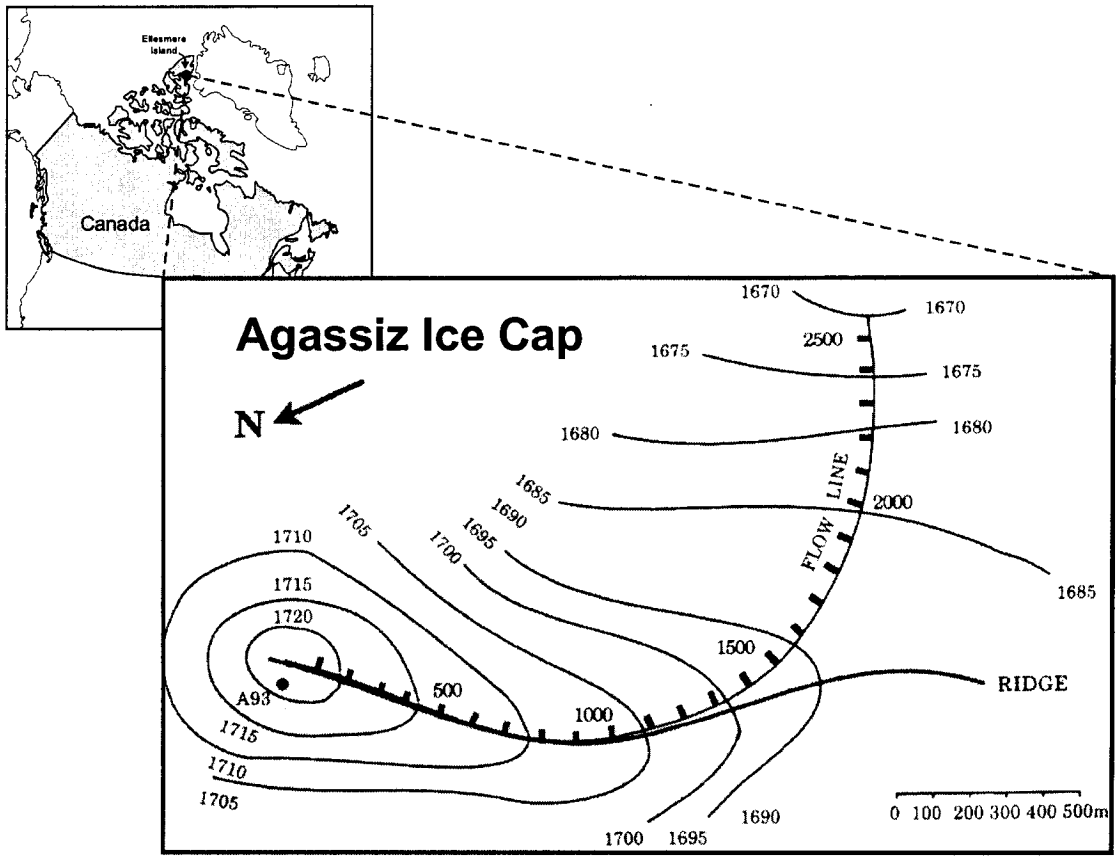

Figure 7 Agassiz ice cap drilling site (modified from Zheng et *al.*, 1998)

2.2 Barnes Ice Cap

Two ice caps are present on Baffin Island in northern Canada: Barnes and Penny ice caps. The Barnes ice cap is of interest to this research and located in the central part of Baffin Island, 69°39'N, 72°39'W (**Figure 8**).

In the Pleistocene distinct large ice caps covered much of the Canadian Arctic Islands, although studies show that ice on Baffin Island was contiguous with the Laurentide Ice Sheet. This massive ice sheet covered most of Canada, with a local spreading center situated in the

Foxe Basin to the west of Baffin Island (Zdanowicz et *al.*, 2002). Barnes Ice Cap was created from the Laurentide ice sheet when its northeastern sector separated from the residual Foxe ice sheet about 6000 ^{14}C years ago. The southeastern section represented today by the Penny Ice Cap was also created during that period.

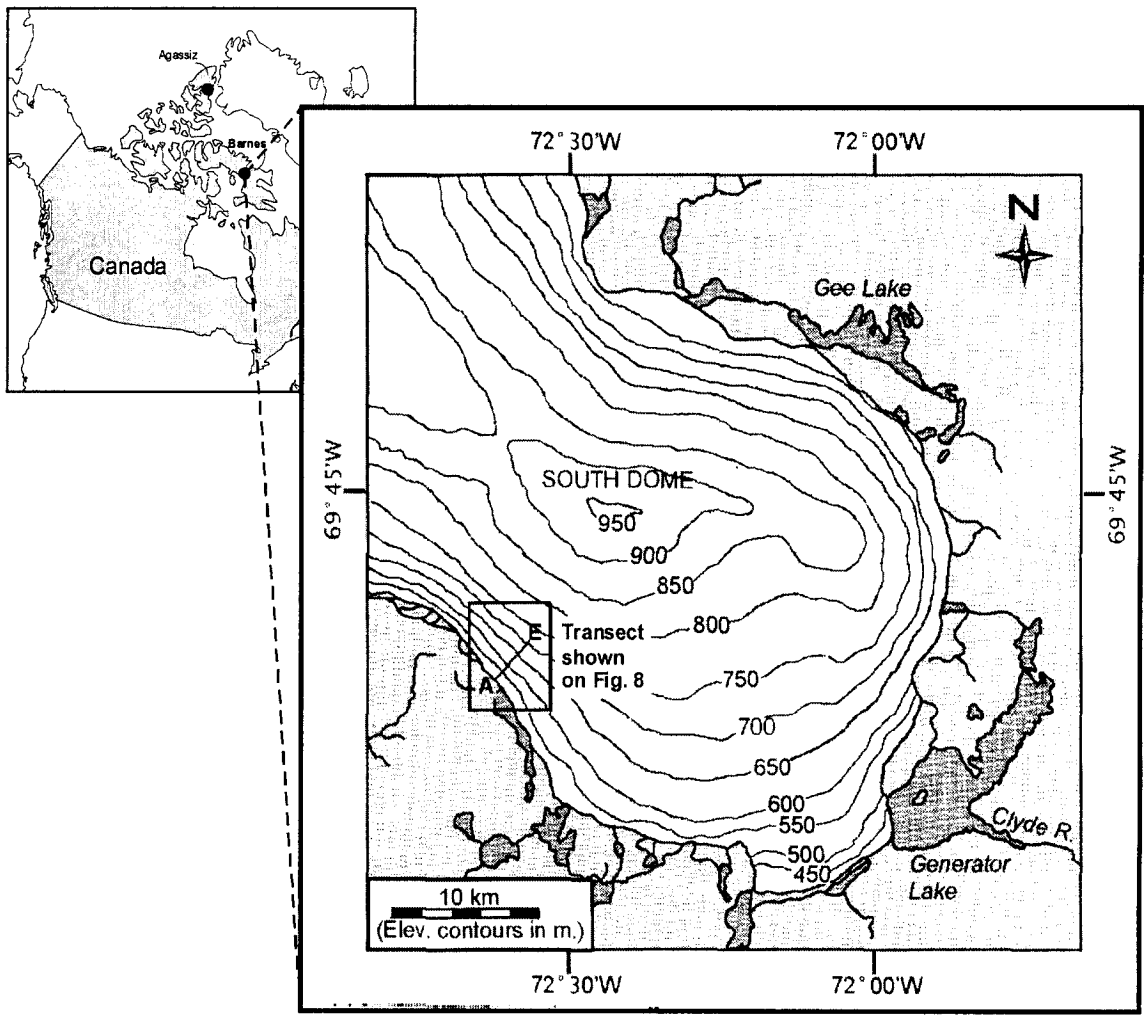

Figure 8 Location of Barnes South Dome and Agassiz (modified from Zdanowicz et *al.*, 2002)

The isotopic content of ice outcropping along the margin of the ice cap, as well as isochrones of deglaciation on Baffin Island provided geological evidence that Pleistocene ice can be found along the margins of Barnes Ice Cap (Zdanowicz et *al.*, 2002). It is the only known site in the Canadian Arctic that allows sampling of Pleistocene ice without deep-coring. Air

photographs provide a distinction between the ice types where Pleistocene ice appears white and is bubble–rich whereas blue ice is bubble-poor and likely formed over the Pleistocene ice during the early Holocene. The margin of the ice cap has an average slope of 12° with the lower 50 m of the margin being filled with rocks debris. Neoglacial moraines are also present. The Pleistocene ice (white ice) is approximately 165 – 180 m wide over a distance of ~ 1 km (Zdanowicz et *al.*, 2002). The glacier lies on mesoproterozoic gneiss.

Sampling at Barnes Ice Cap took place in the summer of 2000 and was performed by the personnel from the GSC. The sampling site is located in the south-western area of the South Dome (Figure 9). It was mainly chosen for its ease of access and a wide exposure of white ice as shown by air photographs. Ice was sampled about 20 cm below the surface using an ice chisel at a distance between 330 m and 400 m from the ice margin (Figure 9). For further information, consult Zdanowicz et *al.*, 2002.

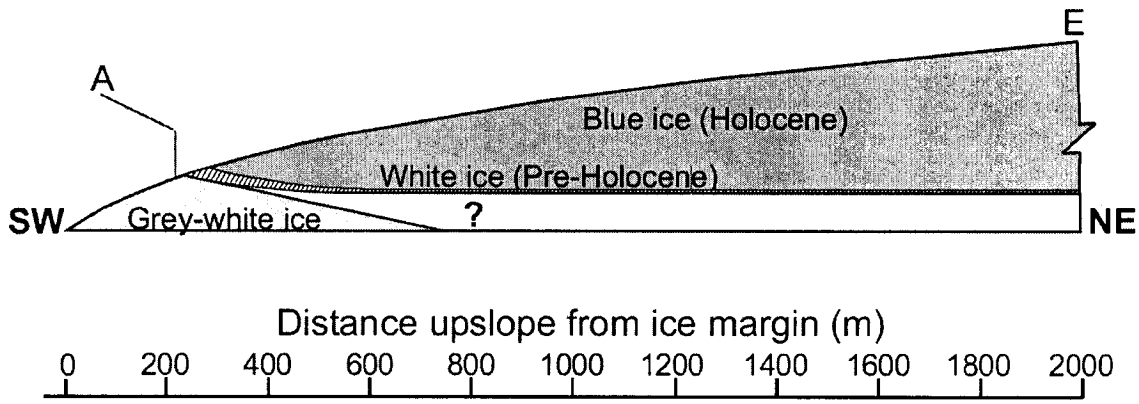

Figure 9 Cross-section of sampled ice on Barnes (modified from Zdanowicz et *al.*, 2002)

2.3 Aufeis Ice

Firth River (68°42'N - 140°00'W) is located on the border of northern Yukon and Alaska (Figure 10). The upper reaches of the river are within the carbonate catchments of the British Mountains and host an extensive area of aufeis ice development. The aufeis ice develops in the Upper Firth River Basin covering an extensive area of 31.5 km^2 with a thickness of between 2.5 and 3 m (Clark and Lauriol, 1997). It is the largest that has been be found in Canada. Topographic maps between 1918 (U.S. Department of the Interior, 1918) and 1983 (Map 117B/9, 1983) show that the ice limits of the aufeis are approximately the same from year to year.

According to the two closest weather stations (Komakuk Beach and Shingle Point), the mean annual temperature ranges between -10 to -12°C. The study site is located about 300 to 400 m higher and roughly 100km from the weather station. Accordingly, it is estimated that the mean temperature at the site is about 2°C lower (Clark and Lauriol, 1997). Precipitation is between 127 and 205 mm/yr.

The river is situated within an extensive region of the northern Yukon that remained outside of the limits of the Laurentide ice sheet during last glacial maximum. It is believed that the Firth River aufeis was first established during the early Holocene when groundwater circulation was increasing due to rising soil temperature and air humidity. About 20% of recharge in the basin is from groundwater (Clark and Lauriol, 1997). In 1991, this represented about 30 mm of groundwater recharge over the Firth River catchments. Redistributing this water over the area underlain by carbonate bedrock would give a recharge

of approximately 100mm for that year. This suggests that about 50% of the runoff comes from groundwater recharge (Clark and Lauriol, 1997).

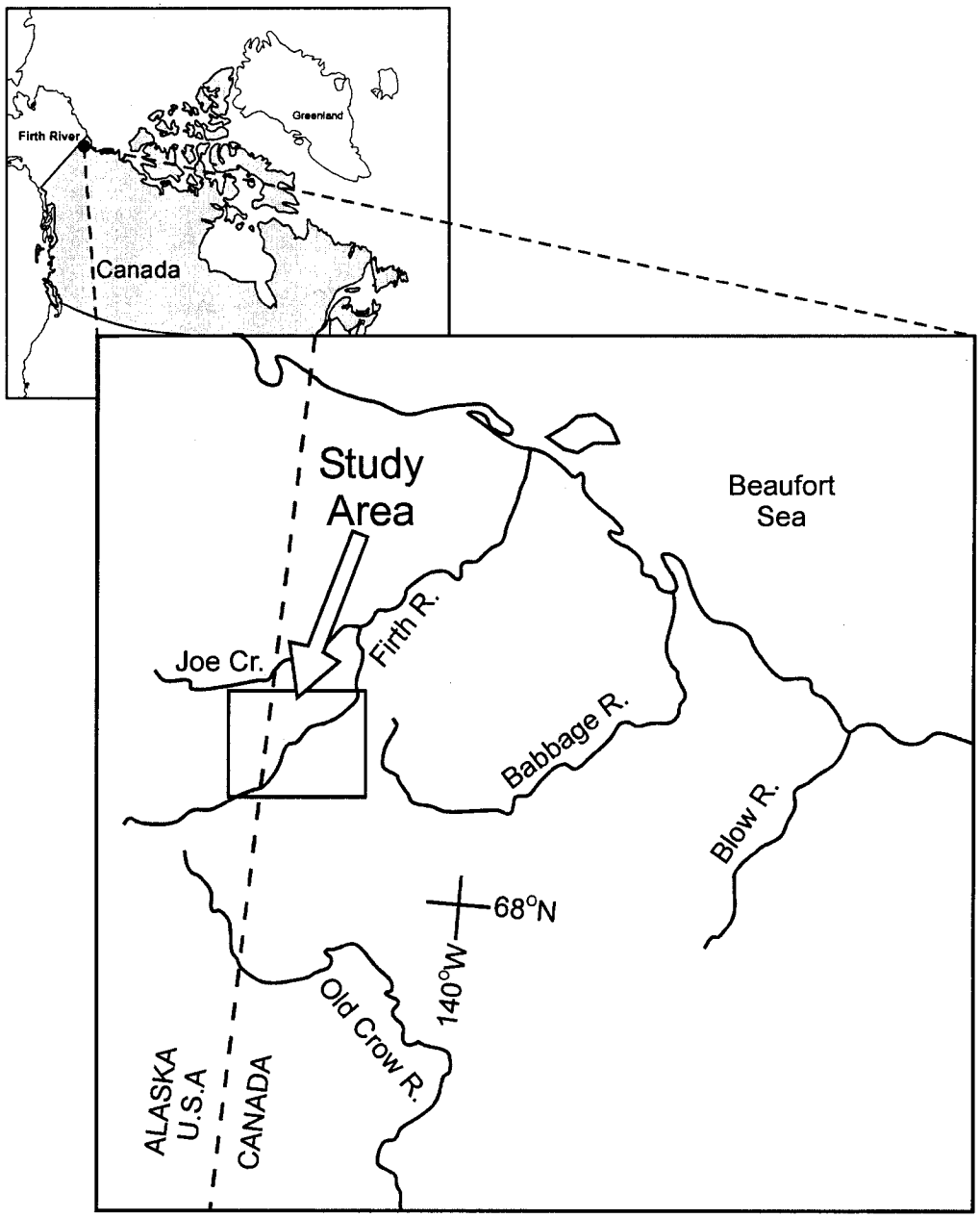

Figure 10 Location of Firth River (modified from Clark and Lauriol, 1997)

The site is located in the continuous permafrost region. Thickness of the permafrost is believed to be as great as 450 m. Vegetation is principally arctic with a forest-tundra ecozone

in the valleys changing to alpine tundra at higher elevations. Above 800 m.a.s.l. vegetation is mostly absent and barren limestone outcrop is found.

The geology of the area is composed of Carboniferous limestone, siliciclastic strata and Proterozoic rocks. These consist mainly of argillites with sandstone and chert of the Neruokpuk Formation and can be found in the northern portion of the Firth River Basin and Joe Creek catchments. Open marine limestone of the Carboniferous Lisburne Group is also present in the upper Joe Creek and upper Firth watersheds. Other rock types found, although less important in coverage, are shales of the Carboniferous Kayak Formation.

Aufeis ice sampling was conducted by personnel from the University of Ottawa in June 1993 on the upper Firth River Basin and in June 1994 in the Joe Creek area (Figure 11). Ice sampled at several locations on the ice landform (FR2-FR3-FR4) using a hand auger was shipped frozen to the University of Ottawa and kept in a freezer until analysis. This location was chosen because of its accessibility and because it drains a considerable carbonate bedrock. For further information, consult Clark and Lauriol (1997).

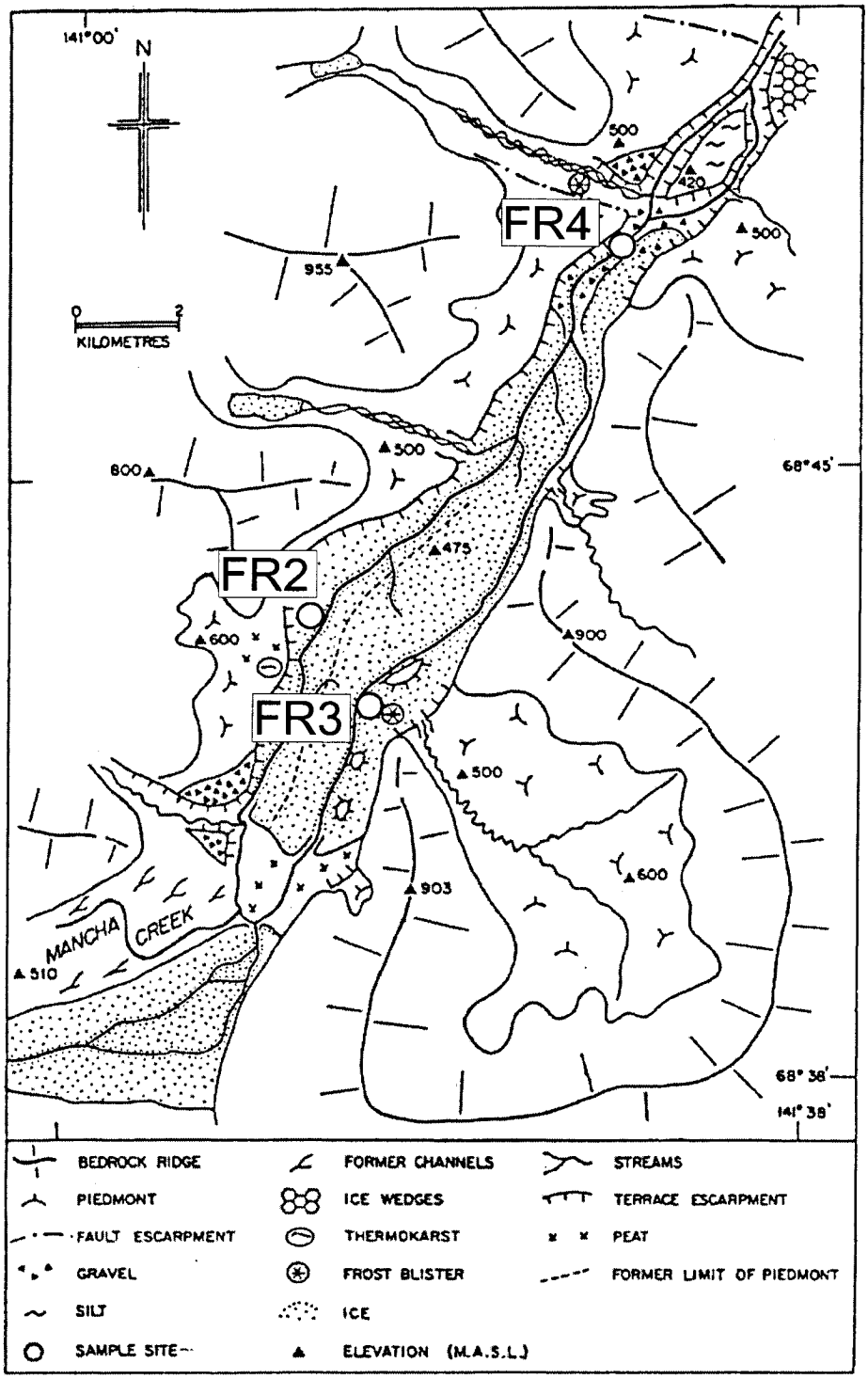

Figure 11 Location of cores from the Firth River area (modified from Clark and Lauriol, 1997)

2.4 Ground Ice

A research site has been established by the Centre d'études Nordiques (CEN), Université Laval, to monitor permafrost in Nunavik, near Umiujap and Hudson Bay in northern Quebec (Figure 12). The site is at an elevation of approximately 185 m a.s.l. and hosts extensive ground ice that contains bubbles and represents a good example of ice with gas bubbles formed by exsolution. The site is currently being studied to determine the hydrological conditions responsible for the formation of ground ice (Fabrice Calmels, 2005 Ph.D. thesis, in preparation).

Northern Quebec was deglaciated about 7000 yr BP (Dyke and Prest, 1987). Following the deglaciation, the Tyrell Sea covered most of the area and the region emerged 6000 yr BP (Lajeunesse and Allard, 2003). It is only since approximately 3,200 yr BP that permafrost began to form in this area (Allard et *al.*, 1987). Discontinuous permafrost is now found throughout the region.

The study site is located in a valley whose surficial geology is composed of post-glacial marine silts and peatland. Beneath the surface layer of mounds are a series of alternating ice layers and sandy silt layers. Some ice layers are as thick as 35 cm. Coarse grained diamicton containing fragments of marine shells is found at a depth of approximately 14 m. These are sediments typically associated with a standstill of the ice front during deglaciation, often observed in the Nastapoka drift belt (Calmels and Allard, 2004).

These sediment types provide conditions necessary for the formation of ground ice. It is believed that the ground ice at this site formed by ice segregation during aggradation of the permafrost. The rate of formation depends on the water supply and the thermal gradient.

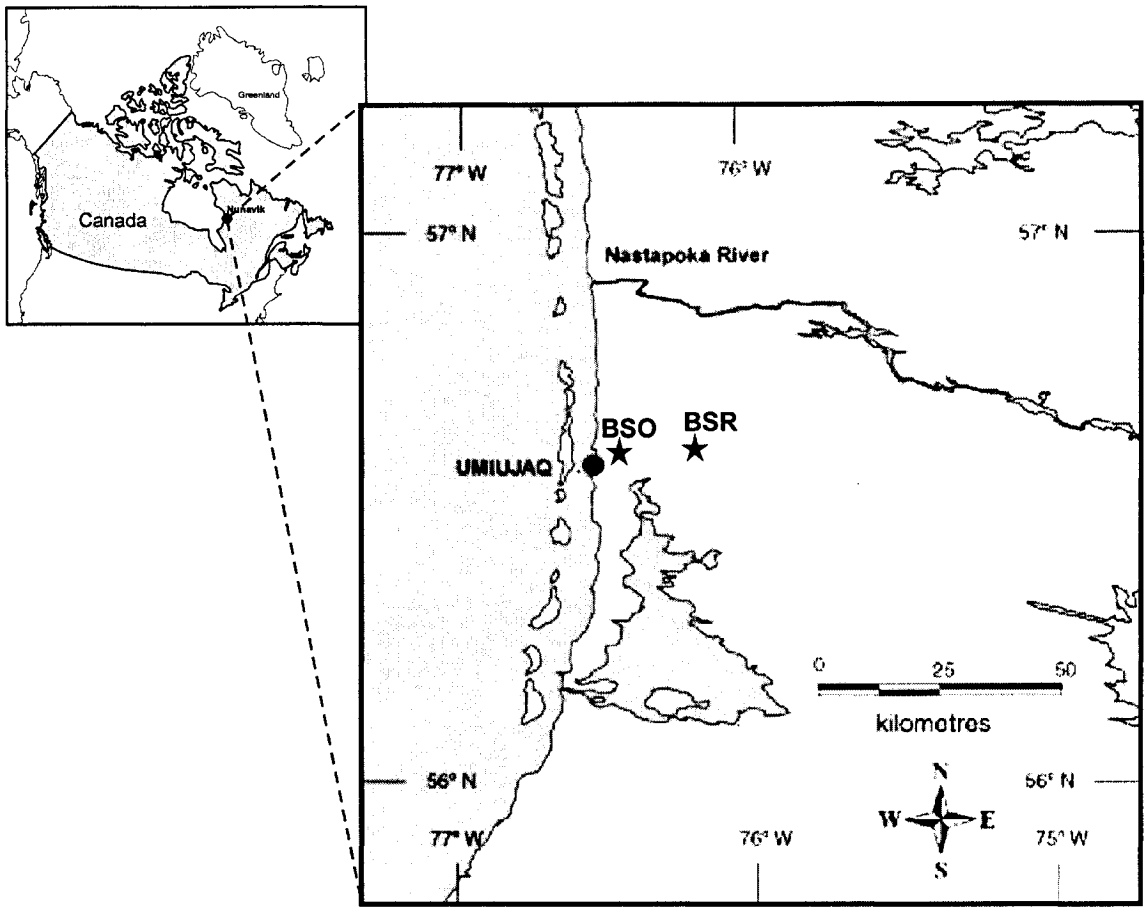

Figure 12 Location of Nunavik, sampling site of ground ice (modified from Calmels and Allard, 2004)

Two lithalsa mounds are of interest to this research, namely BSO and BGR (Figure 2). The area where BGR lays, 56°36.63'N; 76°12.85'W, has been marshland and peatlands for the last 6,000 years BP implying that water supply was optimal for ice segregation and therefore the variations in ice content reflect the variations in the thermal gradient during the growth of those mounds. BSO, 56°33.30'N; 76°28.57'W, and the surrounding lithalsas, are mounds that are approximately 2.5 m high and covered with sand. A lithalsa is a mound formed in mineral soil as opposed to a palsa which is formed in peat but can extend into mineral layers. Ice layers of BSO were formed in silty facies of the glacio-marine sediments that represent a standstill of the ice front during deglaciation.

Sampling of BSO and BGR was performed by personnel representing Centre d'études nordiques (CEN) in July of 2003. Coring was done using a light portable drill designed at CEN. Drilling had been performed at the BGR mound twice before so the hole cored in 2003 was drilled 10 m away from the previous ones. It was cored to a depth of 6.75 m. BSO was sampled for the first time in 2003 and was chosen because the sand cover present is thinner smaller than the active layer which is the upper soil surface that undergoes seasonal freeze-thaw cycles. This situation made it easier to drill with a portable machine. Further information about sampling can be found in Calmels and Allard, 2004.

3 Methodology

The selected methodology for the analysis of the gas trapped in the ice samples collected involves three main steps. First, an ice sample from the field is further cut to remove possible contamination on the outer surface and to be able to fit it in the extraction device. Secondly, the gases are extracted from the ice and transferred into exetainers. Finally, the extracted gas samples are analyzed by mass spectrometry.

3.1 Cutting and storage

The ice is selected for cutting based on its bubble content. Certain types of ice (e.g. Agassiz ice cores) are bubble-rich and therefore pose no problem. On the other hand, ground ice can be bubble-poor and has to be carefully examined to ensure that the ice analyzed will in fact contain gas. Manipulations are performed in a walk-in freezer to prevent melting. Copolymer examination gloves are worn and cores are cut into the desired dimensions (i.e. a square prism 2.5 x 10 cm) using a bandsaw. A thin layer (~ 1 mm) is removed from the ice sample using a clean knife to eliminate any possible impurities introduced from the bandsaw. Any excess snow is also removed with the knife. The cut samples are then individually placed in aseptized « *Nasco* Whirl-pak » bags, properly identified with a sample name and stored in a freezer until analysis. Each sample was analyzed within a week of cutting.

3.1.1 Agassiz

Several analyses have been previously completed on this ice to determine the time scale throughout the cores. Samples analyzed for this project were selected from areas identified as having formed during the Pre-Holocene – Holocene change (Zheng et *al.*, 1998). In total,

eight samples were analyzed from core A93.2 and five samples from core A93.1. Samples from core A93.2 were taken from ice whose depth is of between 107.45 to 109.05 m. Ice between depths of 109 - 113 m was analyzed for core A93.1. Since ice from both these cores is bubble-rich, the ice was simply cleaned and cut in the desired dimension with special attention taken to avoid ice with visible fractures.

3.1.2 Barnes

Four blocks of ice were available for analysis from the Barnes Ice Cap and are named B1, W1, W2 and W3. Distance from the ice margin for each sample was 395.83m, 385.81m, 360.69m and 335.56m respectively. As shown on Figure 9, samples were chosen because they represent the transition zone between pre-Holocene to Holocene. Each block was analyzed 3 or 4 times. No fractures were visible in the ice.

3.1.3 Firth River

The diameter of these cores were not as wide as the glacial ice cores and as a result, had to be cut in two or even three smaller prisms. The samples were selected based on bubble content as bubbles tend to form along lines and not uniformly in the ice. Ice from three cores were analyzed, namely FR2, FR3 and FR4.

3.1.4 Nunavik

Université Laval provided three ground ice samples for analysis. The ice provided was extremely bubble-poor. Bubbles tend to be grouped together along silty clumps which complicated cutting since the bandsaw behaves differently in sediments. A tomodensimeter

showed that the inner walls of the bubbles are covered by a thin sediment layer (Calmels et Allard, 2004).

3.2 Extraction, verification and analysis

Once the ice has been cut, it is ready for extraction and analysis of its gas content. These processes were performed at the G.G. Hatch isotope lab at the University of Ottawa.

3.2.1 Extraction

The following section describes the gas extraction process and refers to the schematic of the extraction line in Figure 13. To begin, the extraction vessel (**D**) is initially cleaned with distilled water, rinsed with acetone and placed in the oven (~ $50\,°C$) to dry for at least one hour. Once dry, the vessel is removed from the oven, cooled to room temperature and finally cooled again in chilled ethanol (~ $-20\,°C$) for 30 minutes. The vessel is now ready to receive ice samples.

The ice is introduced into the vessel using long metal tweezers and wearing copolymer gloves and then the vessel is attached to the extraction line where the sample sublimates for 30 minutes. This process removes any contamination that may have come in contact with the ice during transfer. During sublimation, the vessel is immersed in a hemispherical dewar filled with ethanol chilled to $-20\,°C$ and the line is open to the diffusion pump (**A**). Following sublimation, ice is ready for melting. The valve connecting the vessel to the main line is closed and the flask is immersed in a beaker containing warm water in order to accelerate the melting of the ice. During melting, the gas is liberated from the ice into the headspace. Once

all the ice is melted, the bottom of the vessel is slowly chilled with a -70 °C ethanol bath. The water freezes from the bottom to the top, allowing gases still dissolved in the water to be exsolved into the headspace. Once the ice is completely frozen, the flask is immersed in a -100 °C ethanol bath for 15 minutes to ensure equilibrium has been reached. The gas sample is then ready for its first transfer. A stainless steel tube attached to the line (**E**) is inserted in a liquid Helium dewar. After closing the valve connecting the line to the vacuum, the valve connecting the vessel to the line is open and gas is allowed to expand in the extraction line. After a minute, the valve connecting the stainless steel tube to the line is open and the gas becomes trapped into this tube. The melt-refreeze process is repeated a second time to transfer gas that might not have escaped during the first melt-freeze process. By observing the pressure gauges (**B** and **C**), we are able to confirm that the gas sample has been transferred into the tube when pressure returns to pre-expansion values.

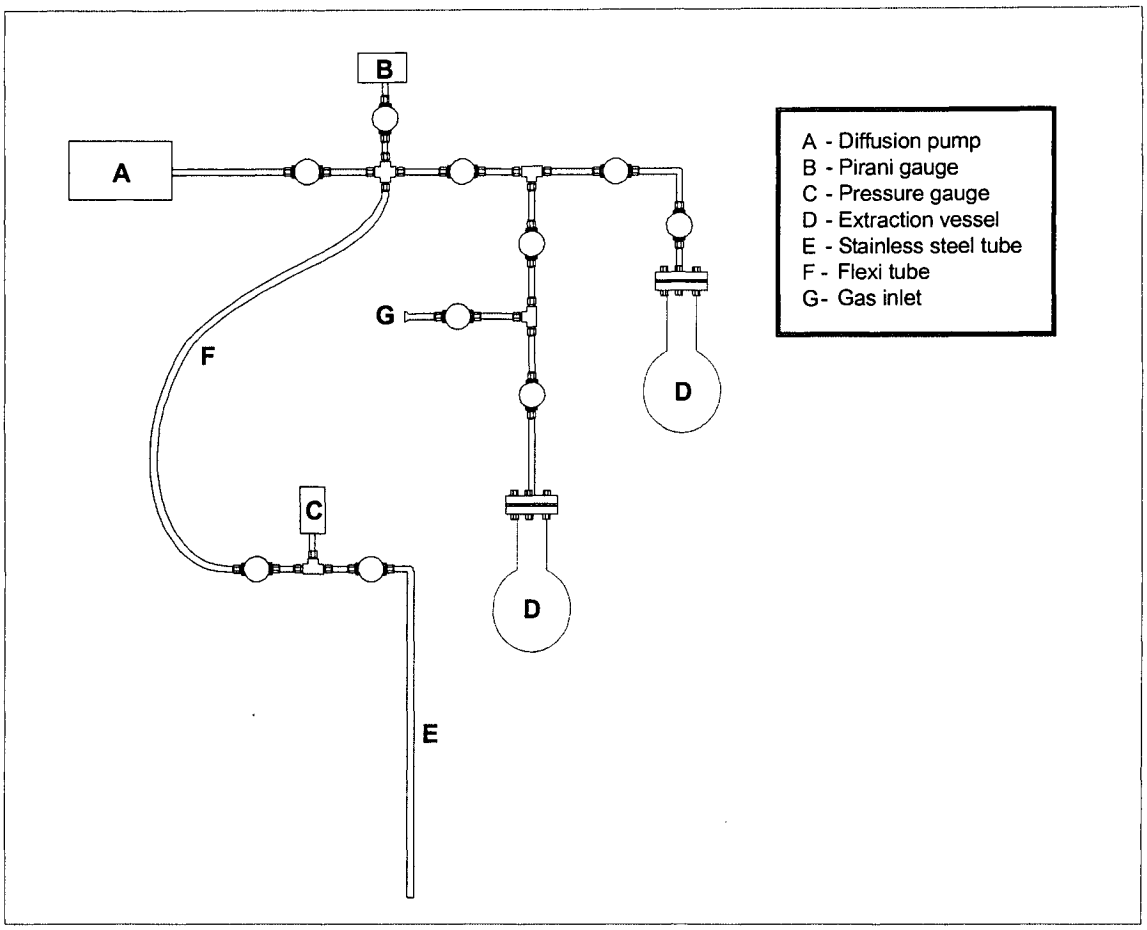

Figure 13 Schematic of the gas extraction line

The stainless steel tube is then left room temperature for 45 minutes. After this that, the gas is transferred in an empty 12 ml borosilicate exetainer equipped with a screw cap and pierceable rubber septum (Figure 14) using helium as a transport gas.

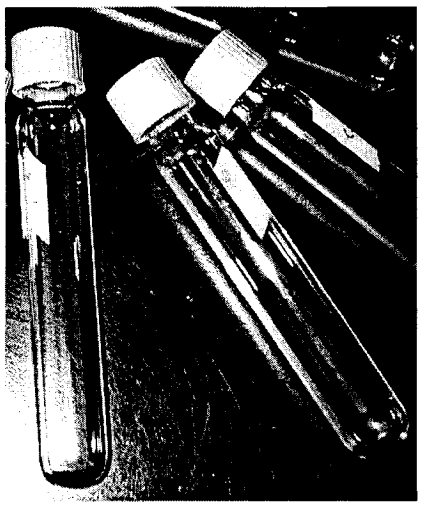

Figure 14 exetainers

3.2.2 Mass spectrometry analysis

Samples were analyzed on a Thermo Finnigan Delta^{plus} XP for continuous flow isotope ratio mass spectrometry with an eight special collector assembly coupled with a GasBench II with Restek model RT-Msieve 5A (30m length, 0.32mm internal diameter) for sample transfer. Gas samples are introduced into the GasBench by helium transport. They initially go through a process of water removal before entering the Restek column. Here a 100 μL aliquot of the sample is taken and then transferred into the gas chromatograph (GC) column where the gases are separated depending on their polarity.

All the gases have a unique retention time and therefore exit this column at different periods allowing the mass spectrometer to analyze one gas at a time. The gases then go through another phase of water removal before entering the ion source where all the particles are ionized. Following this step the ionized particles enter the magnetic field where they will be separated by mass, into the different collectors. We use a peak jump to measure N_2 because it

uses the same collectors as O_2. Three reference gases are also measured every time for Ar, N_2 and O_2 for isotopic ratios measurement.

3.2.3 Verification of method

A leak check of the extraction was routinely performed by closing the valve connecting the manifold to the pump and verifying that the pirani gauge remained constant. A slight increase is always observed due to degassing but stabilizes at approximately 10^{-4} mTorr.

A blank test was also performed daily on the transfer line to ensure that no measurable background gases accumulated in the line. To accomplish this, the line is pumped for at least 10 minutes after which the residual gases in the line are transferred to an exetainer for measurement on the mass spectrometer. Results for these tests indicated that no measurable background gases accumulate in the line.

Occasionally a blank test to verify background gases was performed on the extraction line by following the steps mentioned in 3.2.1 and 3.2.1 but without introducing any ice to the vessel. This process is very time consuming and consequently was only performed a limited number of times. However for each instance, the line proved to be uncontaminated.

Yet another means of testing the integrity of the extraction line involved using a compressed air standard to ensure consistency of the extraction. Isotopic results for the six compressed air standards completed can be seen in Figure 15. The value of $\delta^{18}O$ has a standard deviation of 0.443 and for $\delta^{15}N$ of 1.750 but if the outlier is removed, the standard deviation becomes 0.186. The outlier was caused by a change in flow of the standard N_2 gas.

The compressed air standard was also introduced in degassed ice within the extraction vessel to ensure stability and precision of the method. This process involved introducing a few fabricated ice cubes in the vessel and removing their gas content by a series of 2 melt-refreeze cycles.

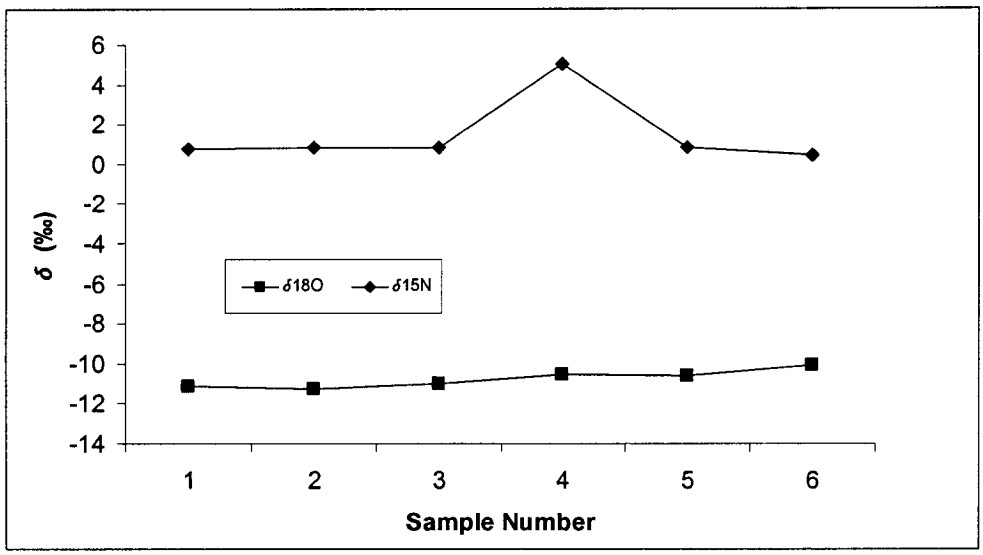

Figure 15 Isotopic content of oxygen-18 and nitrogen-15 in compress gas. The x-axis represents the sample trial number and the y-axis represents the delta isotopic ratio (‰).

Afterwards, compressed air was introduced in the line and an aliquot was trapped in the extraction vessel. Normal extraction procedures follow. Results shown in Figure 16 indicate that the $\delta^{18}O$ has a standard deviation of 0.09 and the $\delta^{15}N$ of 0.13. A difference is noticeable (Table 4) in the isotopic content between the compressed air (Figure 15) and the compressed air in degassed ice (Figure 16). This difference was expected due to the method of introducing the compressed gas into the vessel. Since the vessel is at approximately -100°C, there is a temperature induced fractionation of the isotopes. The heavier isotopes of oxygen tend to accumulate at the colder temperature, creating a less depleted ratio. Since O_2 has a smaller diameter than N_2, it diffuses faster, which is why the difference is more noticeable in

$\delta^{18}O$ (Craig et *al.*, 1988). The values of $\delta^{15}N$ are too close to discern a difference between compressed air and compressed air introduced in degassed ice.

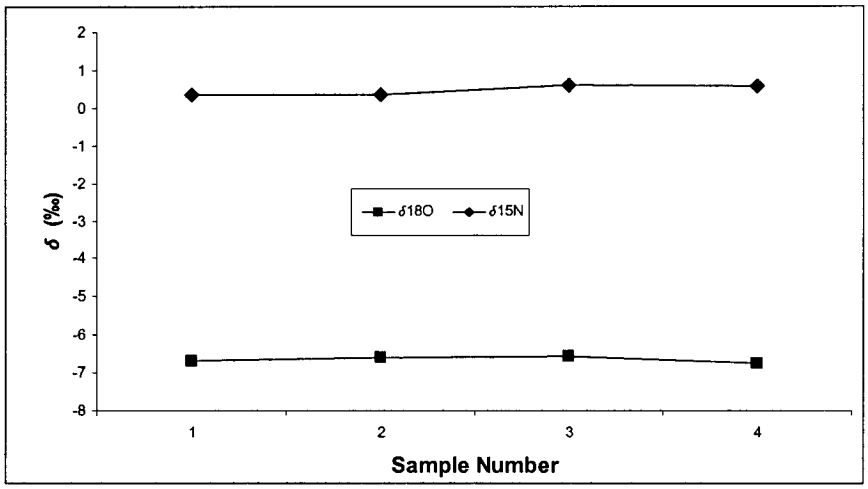

Figure 16 Isotopic content of oxygen-18 and nitrogen-15 compressed gas in degassed ice. The x-axis represents the sample number while the y-axis represents the isotopic values (‰).

Table 4 Comparison between isotopic content in compressed air and compressed air introduced in degassed ice. Note that the $\delta^{15}N$ outlier was removed in the compressed air.

Trial #	$\delta^{18}O$ (‰)		$\delta^{15}N$ (‰)	
	compressed air	compressed air in degassed ice	compressed air	compressed air in degassed ice
1	-11.1554	-6.6817	0.8013	0.3588
2	-11.2315	-6.6025	0.8405	0.3568
3	-10.9654	-6.5649	0.8175	0.5903
4	-10.5198	-6.7657		0.5842
5	-10.5959		0.8618	
6	-10.0699		0.4170	
average	-10.7563	-6.6537	0.7476	0.4725
standard deviation	0.4431	0.0891	0.1862	0.1325

Finally a standard gas consisting of air taken outside in a glass container on October 19th, 2004, was measured 9 times in order to provide values for correction of isotopic values. This reference gas also allowed verification of reproducibility of extraction and analysis on the mass spectrometer. As seen in Figure 17, isotopic ratios are constant and both average at approximately 0 ‰.

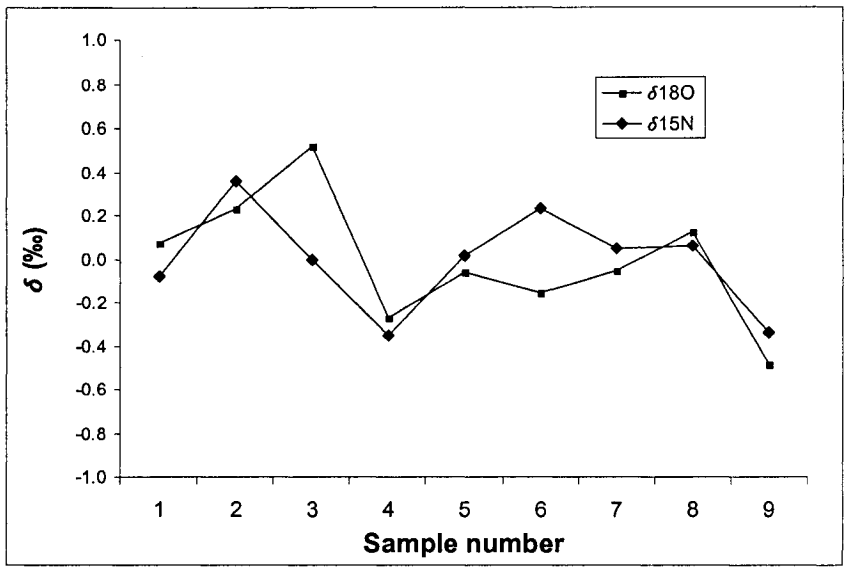

Figure 17 $\delta^{18}O$ and $\delta^{15}N$ values as measured in the standard gas.

3.2.4 Analytical consideration

The extraction and analytical method described in 3.2.1 and 3.2.2 used a standard gas to verify the extraction and analysis procedures. Nonetheless, deviation in isotopic values and gas ratios must be addressed.

Table 5 presents the results of standard trials indicating that both $\delta^{18}O$ and $\delta^{15}N$ values are close to zero, which in turn indicates that the gas is precise and reproducible. The average $\delta^{18}O$ is –0.0091 ‰ with a standard deviation of 0.29 while the average value of $\delta^{15}N$ is –0.0064 ‰ with a standard deviation of 0.23. The precision for $\delta^{18}O$ is ± 0.67 and for $\delta^{15}N$, ± 0.54. Because of the precision of the isotopic measurements, it might prove difficult to differ between gas content of glacial and interglacial in glacier ice cores.

Another important aspect to consider is the precision of the gas ratio measurements. Gas ratios of N_2/Ar and O_2/Ar, as displayed in Figure 18 and Table 5, are similar to atmospheric ratios. The average molar ratio O_2/Ar and N_2/Ar of the working standard are 22.43 and 83.60

respectively with standard deviation of 0.58 and 83.60. These values are equal to the value found in the atmosphere indicating gas ratio measurements are accurate for the method.

Table 5 Isotopic and molar gas ratios results of the standard gas

Standard	$\delta^{18}O$ (‰)	$\delta^{15}N$ (‰)	O_2/Ar	N_2/Ar
1	0.0702	-0.0814	23.2542	79.1791
2	0.2308	0.3618	23.0937	77.0468
3	0.5179	-0.0004	22.7182	72.6509
4	-0.2707	-0.3505	22.0272	74.0258
5	-0.0624	0.0136	21.5612	86.1006
6	-0.1541	0.2297	22.2381	88.9197
7	-0.0544	0.0486	22.1303	92.2314
8	0.1241	0.0586	21.9121	91.3872
9	-0.4831	-0.3375	22.9002	90.8738
average	-0.0091	-0.0064	22.4261	83.6017
standard deviation	0.2912	0.2325	0.5848	7.8791

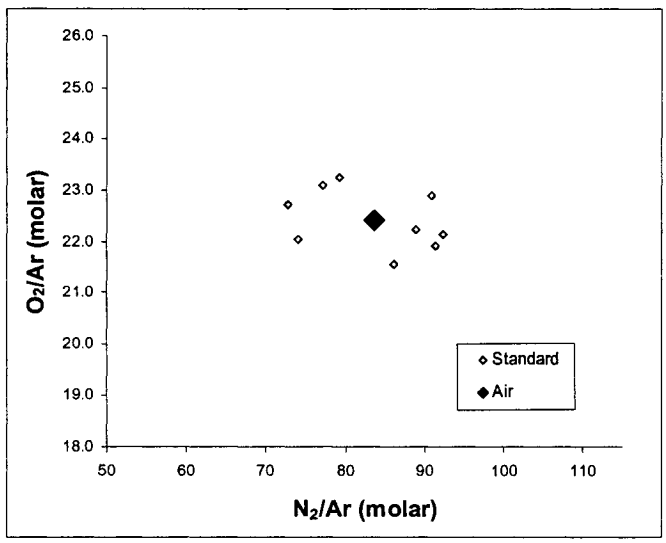

Figure 18 Comparison of the gas ratios in the working standard with the atmospheric values

4 Results - Gases in glacier ice

Use of glacier ice samples in this research is essential for establishing the molar and isotopic ratios of gases trapped in ice that are essentially atmospheric in origin. Results from the Barnes and Agassiz ice are summarized and compared in the following section. Gases entrapped in both glaciers are accepted as atmospheric gas with no dissolution or exsolution. However, modification of both molar and isotope ratios from a primary atmospheric signal can be anticipated due to the diffusion and entrapping processes of gases in firn described in section 1.3.1.

4.1 Agassiz

Isotopic content and gas ratios are compiled in Table 6 for the Agassiz ice samples. Note that some isotopic values of oxygen in Table 6 were removed due to erroneous values resulting from a change in reference gas for the mass spectrometer.

The results for O_2/Ar ratio are similar for both cores, with an average of approximately 22.5 and a low standard deviation. The results for N_2/Ar ratios are slightly different, typically 86.35 in core A93.2 and higher in core A93.1 at 88.14. The standard deviations are higher for N_2/Ar than for O_2/Ar. Both O_2/Ar and N_2/Ar ratios are lower in core A93.2. Results for O_2/N_2 are constant and show a low standard deviation. As seen in Figure 19, the O_2/Ar and N_2/Ar ratios in Agassiz ice are marginally higher than atmospheric values.

Table 6 displays that $\delta^{18}O$ values are higher in 93.1 than in 93.2 with averages of 1.98‰ and 0.56‰, respectively. The samples analyzed from those cores came from different depths.

Isotopic values of nitrogen are similar in both cores, although the average value of $\delta^{15}N$ in 93.1 is 0.3 ‰ higher than in 93.2.

Table 6 Molar ratio and isotope data for entrapped gases from Holocene and Pleistocene Agassiz ices cores

Core - sample number	Approximate depth	$\delta^{18}O$ (‰)	$\delta^{15}N$ (‰)	O_2/Ar	N_2/Ar	O_2/N_2
			Agassiz 93.2			
145 - 2	107.45m - 107.91m	0.2282	-0.0168	22.0334	82.5811	0.2644
145 - 3	107.94m - 108.04m		0.0804	22.1571	86.1663	0.2549
146 - 4	108.04m - 108.14m	1.0133	0.4798	23.2384	84.7776	0.2717
146 - 6	108.24m - 108.34m		0.5894	22.3223	83.2443	0.2658
146 - 7	108.34m - 108.44m	0.3479	0.2371	22.2602	84.7846	0.2602
146 - 8	108.44m - 108.60m		0.9051	23.0144	91.4909	0.2493
147 - 9	108.60m - 108.70m	0.6580	0.8290	22.6058	88.3066	0.2537
147 - 11	108.80m - 108.90m		0.5245	22.1765	89.4300	0.2458
	average	0.5619	0.4536	22.4760	86.3477	0.2582
	standard deviation	0.3513	0.3330	0.4384	3.1293	0.0088
			Agassiz 93.1			
132 - 1	109.87m - 109.97m	1.7212	0.2963	23.5879	88.1347	0.2653
132 - 2	109.97m - 110.07m	2.2674	0.7694	22.5692	90.9547	0.2459
135 - 2	111.72m - 111.82m	1.1137	0.7888	22.0974	88.8488	0.2465
135 - 3.1	111.82m - 111.92m	1.7000	0.9712	22.3307	87.2859	0.2536
135 - 3.2	111.82m - 111.92m	3.1116	0.9569	22.6156	85.4979	0.2622
	average	1.9828	0.7565	22.6402	88.1444	0.2547
	standard deviation	0.7515	0.2735	0.5688	2.0084	0.0088

Generally, heavy gases become enriched after an extended residence time in the diffusive zone of the firn air column (Craig et *al.*, 1988), which would be expected in Agassiz ice. However, during the sublimation stage of the extraction (refer to chapter 3), most of the samples fractured into smaller pieces, suggesting the occurrence of microfractures as stated by Sowers and Bender (1989). No other samples of ground ice, aufeis ice or ice from Barnes glacier that were analyzed fractured during the extraction process.

Previous work done by Sowers and Bender, 1989, suggest that cracks in ice, whether microfractures or cracks induced during recovery of the ice core, result in gas loss processes that may alter gas composition. It was suggested that gases with a smaller diameter, such as Ar, are lost faster than those with larger diameter (Craig et *al.*, 1988) which would result in higher O_2/Ar and N_2/Ar ratios. Since the ice samples fractured during the extraction process,

there is a possibility that the ice contained weak points within the ice likely due to microfractures. Consequently during sublimation in the extraction vessel, part of the argon (smaller diameter) in the bubbles connected to micro fractures may have been lost, and the gases remaining in the ice would have higher ratios, as observed in Figure 19.

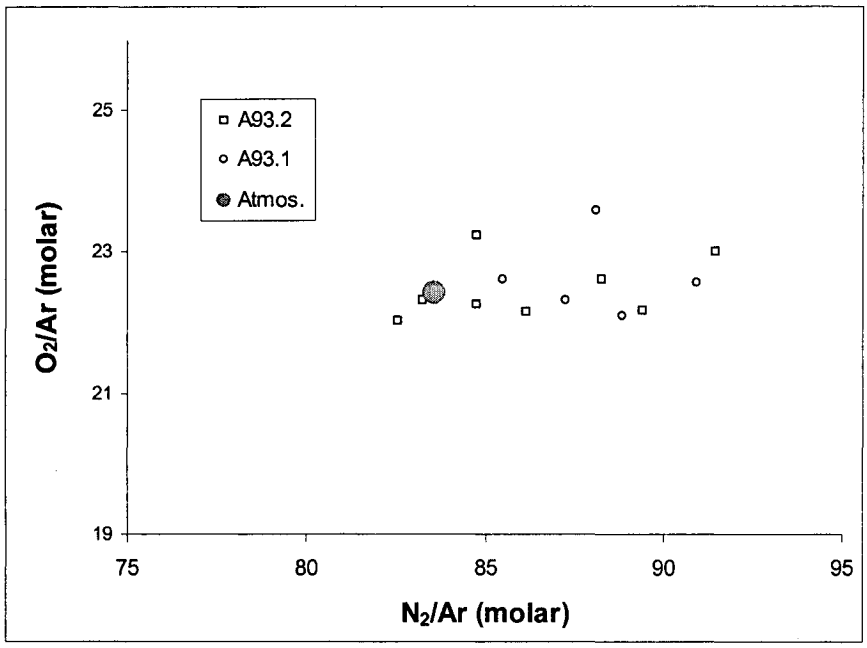

Figure 19 Gas ratios in Agassiz ice cores expressed as molar ratios

Comparing the isotopic content of Agassiz with standard values (Figure 20) suggests that the average value of both Agassiz cores are more enriched in ^{18}O and ^{15}N than in the standard. This implies that gravitational fractionation occurred during entrapment of gas in the firn, which may have preferentially caused the heavier isotopes to be trapped in the ice (Craig, H. et *al.*, 1988). The average enrichment in ^{18}O usually has a range between 0 and 0.82 ‰ during the Holocene (Sowers and Bender, 1989; Caillon et *al.*, 2003) and between 0 and 1.25 ‰ during Pleistocene (Bender et *al.*, 1994). Thus, it appears that the isotopic values in Agassiz are more enriched than what would be expected. This over-enrichment could also be attributed in part to the microfractures thought to be present in the Agassiz cores.

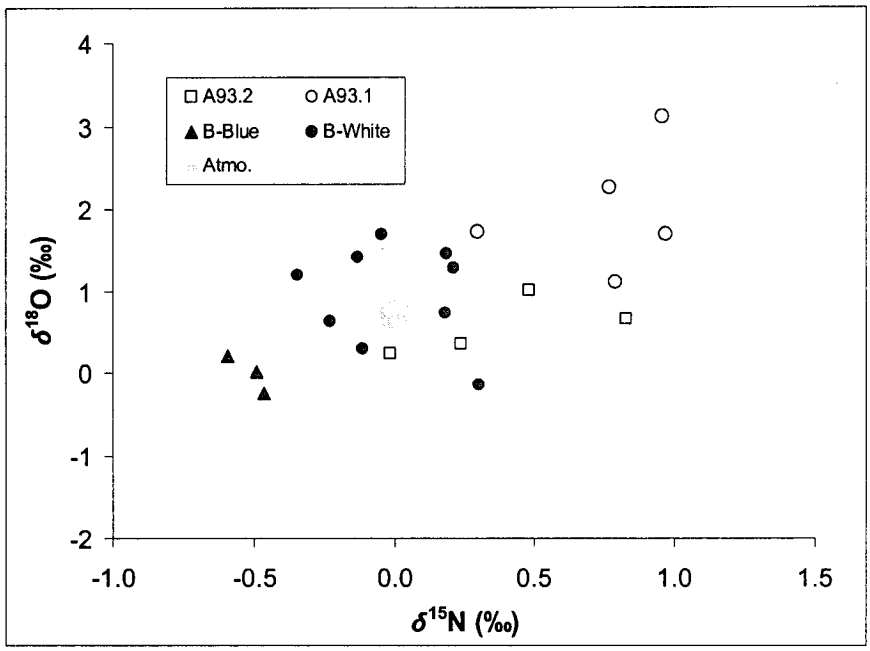

Figure 20 Isotopic result of oxygen-18 and nitrogen-15 of the air trapped in bubbles in Agassiz and Barnes ice cores

Comparison of the isotopic content and the solid electrical conductivity of ice as a function of depth (Figure 21), reveals a small increase in $\delta^{18}O$ and $\delta^{15}N$ as depth increases. Previous work done on Agassiz ice cores revealed that in A93.1 and A93.2, a depth 108.6 m corresponds to an age of approximately 11,550 years before present (personal communication with David Fisher, 2004). This age represents the time when the most recent deglaciation was initiated, i.e. the change from Pleistocene to early Holocene. Higher isotopic ratios of oxygen-18, such as those found deeper than 108.60m, are associated with a colder period, i.e. pre-Holocene (Bender et *al.*, 1994). This trend suggests that the data obtained from the gases from this research also confirms the change from Pleistocene to Holocene but that there is a gas-ice age difference.

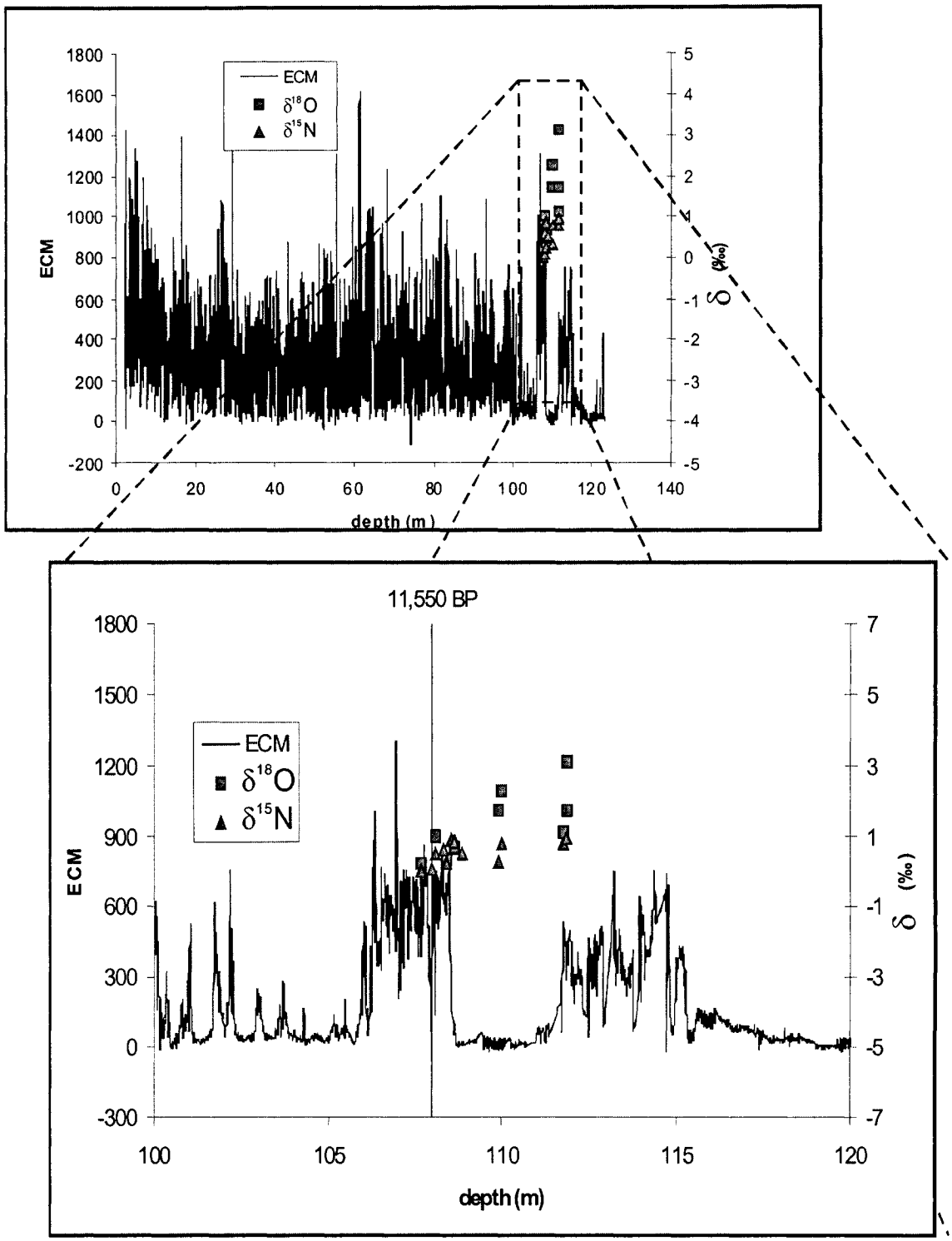

Figure 21 Comparison of solid electrical conductivity (ECM) and measured isotopic values in Agassiz ice core A93.1 and A93.2. The data has been modified from Zheng et *al.*, 1998. The lower graph is a closer view of the depth sampled for this research.

4.2 Barnes

Gas ratios and isotopic content are presented in Table 7 for the samples from the Barnes ice cap. The values of nitrogen for sample W3.1 are discarded because of a flow problem encountered during analysis on the mass spectrometer.

Table 7 Molar ratio and isotope data for entrapped gases from Barnes ices cores

Sample #	$\delta^{18}O$ (‰)	$\delta^{15}N$ (‰)	O_2/Ar	N_2/Ar	O_2/N_2
		Barnes Blue			
B1.1	-0.2535	-0.4644	19.7595	77.3237	0.2533
B1.2	0.2102	-0.5912	19.8799	76.6669	0.2570
B1.3	0.0129	-0.4885	20.3532	76.3040	0.2644
Average	-0.0102	-0.5147	19.9975	76.7648	0.2582
Standard deviation	0.2327	0.0673	0.3138	0.5168	0.0056
		Barnes White			
W1.1	-0.1411	0.3017	19.6460	77.2372	0.2521
W1.2	1.4110	-0.1297	19.8698	77.1636	0.2552
W1.3	1.1931	-0.3431	19.1271	75.8044	0.2501
W1.4	1.4620	0.1877	17.2155	82.4646	0.2069
W2.1	1.6987	-0.0475	19.8283	77.7203	0.2529
W2.2	1.2797	0.2120	19.6532	76.2106	0.2556
W2.3	0.6305	-0.2291	17.3531	79.3685	0.2167
W3.1	0.8098		19.1282		
W3.2	0.7353	0.1805	18.8218	78.7121	0.2370
W3.3	0.2848	-0.1156	18.3925	81.0981	0.2248
Average	0.9364	0.0019	18.9035	78.4199	0.2390
Standard deviation	0.5775	0.2254	0.9732	2.2278	0.0186

The values of O_2/Ar and N_2/Ar are similar between the B-Blue and B-White ice blocks, with averages of approximately 19 and 78, respectively. Generally, the ratios in B-Blue ice appear more constant than those from B-White ice. In particular, N_2/Ar of B-White has ratios ranging from 75.8 to 82.5. Although the isotopic values of oxygen-18 are fairly consistent in both ice blocks, those in B-Blue are significantly lower than those in B-White. An increase in $\delta^{18}O$ from W3 to W1 was observed. Results for $\delta^{15}N$ oscillate around zero for both B-Blue and the B-White.

Comparing O_2/Ar and N_2/Ar ratios in Barnes ice (Figure 22), suggests that both ratios are lower than present atmospheric values. Craig et *al.* (1988) report that there is enrichment in heavy gases during the entrapment of atmospheric air in the firn. The Barnes ice cap was previously part of the Laurentide ice sheet which implies a colder environment at higher altitude than present day conditions. Colder temperatures imply a longer residence time in the diffusive layer resulting in the enrichment of the heavy gases such as argon which explains the low ratios observed.

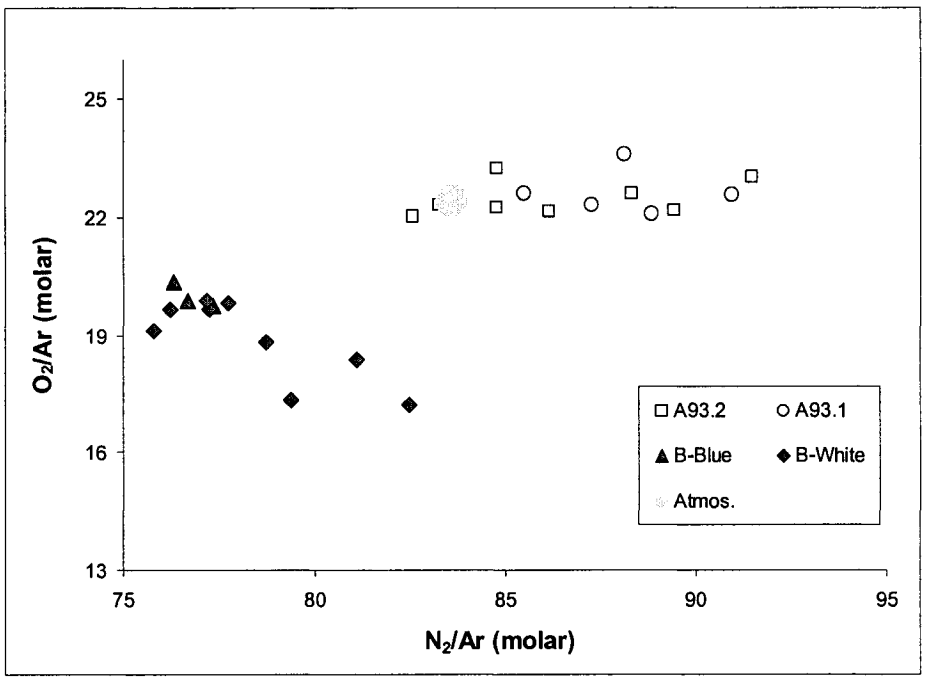

Figure 22 Comparison of O_2/Ar and N_2/Ar gas ratios in Agassiz and Barnes ice cores

Zdanowicz et *al.* (2002) discovered the presence of Pre-Holocene and Holocene ice at Barnes. The samples analyzed as part of this research fall within the transition zone between Holocene and pre-Holocene ice. As seen in Figure 23, at distance of 395 m from the ice margin, the $\delta^{18}O$ of the ice is increasing while the $\delta^{18}O$ of the gas is decreasing. A decrease in the $\delta^{18}O$ of

the ice previously occurred starting at a distance of 380m from ice margin. It is believed that this offset is a result of the difference in the age of the ice and the age of the gas. For the Devon Island ice cap, the offset is on the order of 85 years (Henderson et *al.*, in review). It is accepted that blue ice was formed during the Holocene, while white ice holds a record of pre-Holocene ice (Zdanowicz et *al.*, 2002). Analysis of the B-Blue samples in this research placed them in the transition zone, and therefore this ice cannot be classified as Holocene ice.

Figure 20 displays a comparison between changes in the isotopic content of Barnes ice and present day atmosphere. The average $\delta^{18}O$ of O_2 for the B-White ice block, considered as pre-Holocene, is enriched by almost 1 ‰ with respect to present day atmosphere. This is expected due to its age (Bender et *al.*, 1994). On the other hand, the average $\delta^{18}O$ of O_2 for B-Blue ice, considered as early Holocene ice, has a similar isotopic content as present day atmosphere. Isotopic content from Holocene would be expected to have an enriched ratio of 0 ‰ – 0.8 ‰ with respect to present day atmosphere (Sowers and Bender, 1989; Caillon et *al.*, 2003). Since the transition between pre-Holocene and Holocene begins with a general decrease in the isotopic content of the $\delta^{18}O$ of the ice followed by an increase (Figure 23), the same can be expected of the $\delta^{18}O$ of O_2.

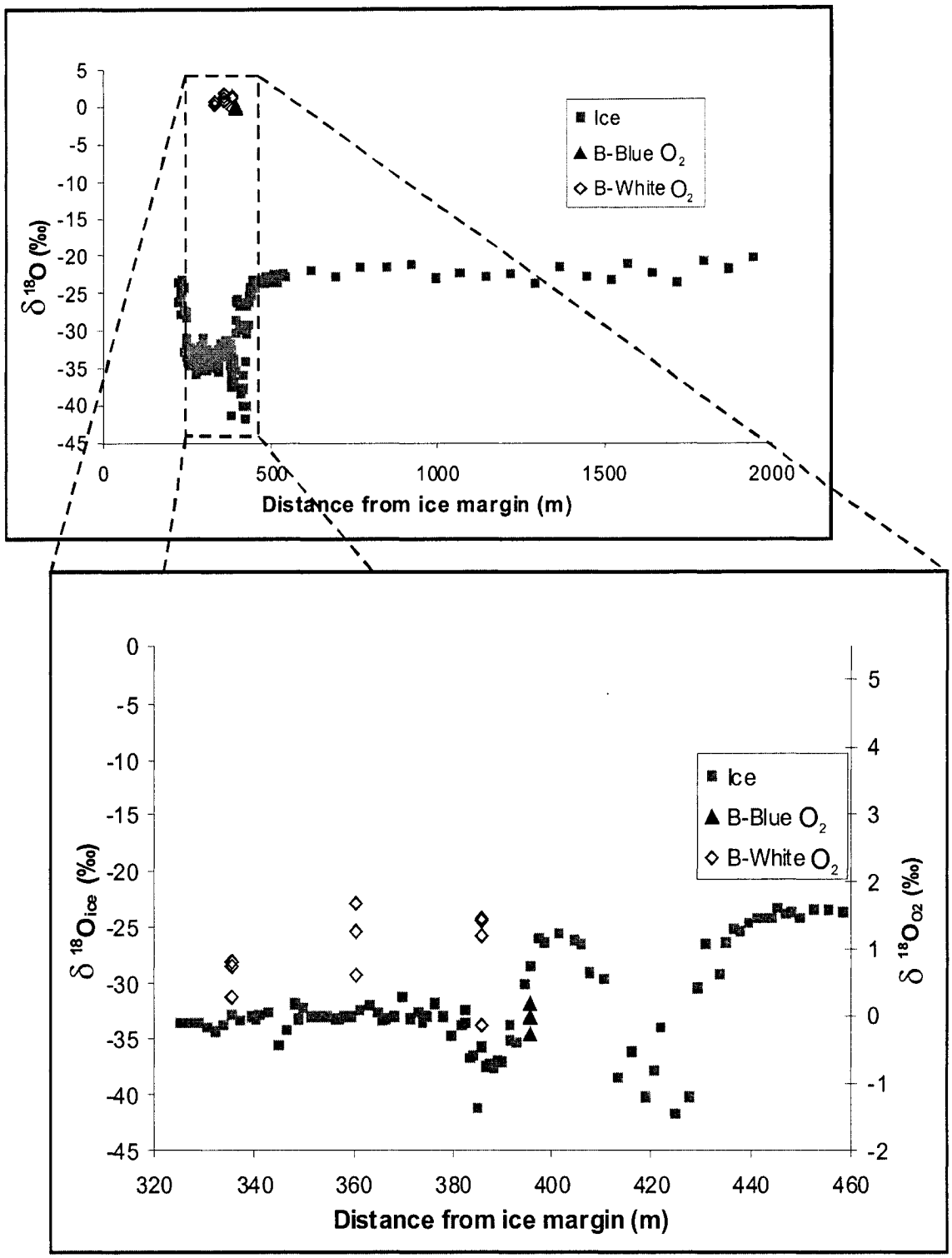

Figure 23 Isotopic content of oxygen-18 of Barnes ice compared with oxygen-18 content of gases trapped in bubbles in Barnes ice. The x-axis represents the distance from the glacier margin and the y-axis reflects the oxygen-18 content in the ice and in the gas. The lower graph is a closer view of the depth sampled for this research.

4.3 Synthesis – glacier ice

The Agassiz and Barnes ice cores indicate that both glaciers show distinct O_2/Ar and N_2/Ar ratios (Figure 22). Values from Barnes have a strong negative correlation with a coefficient of –88%, while the coefficient for the Agassiz data is not as strong and tends to be positive with a value of 25%. Generally, N_2/Ar and O_2/Ar ratios are more enriched for Agassiz than they are for Barnes. The smaller gas ratio values in Barnes suggest either enrichment in argon. Agassiz is consistent with the standard values of O_2/Ar but displays enriched values for N_2/Ar in comparison with the standard values.

The difference observed between both glaciers is most likely a result of different conditions of accumulation and/or storage conditions for Agassiz ice. Barnes, being part of the Laurentide ice sheet, accumulated ice under colder conditions at high latitude on the eastern spreading center which promoted a thicker diffusive air column. This affected the isotopic content by gravitational fractionation and its gas ratios by gravitational settling. In the case of Barnes, O_2/N_2 is still very similar to standard values, suggesting that argon probably increased before occlusion in air bubbles, hence the enrichment in heavy gases (Sowers and Bender, 1989; Caillon et *al.*, 2003). Agassiz is located further north than Barnes and was not part of a continental ice sheet and was therefore at a higher latitude but lower altitude than Barnes. Gas ratios in Agassiz could also be affected by microfractures.

As shown in Figure 20, isotopic ratios also vary between the Agassiz and Barnes ice. Generally, it can be observed that $\delta^{15}N$ values are more enriched in Agassiz than they are in Barnes. A slight increase in $\delta^{15}N$ is also associated with a slight increase in $\delta^{18}O$. Although samples from both glaciers were taken from a depth representing a change between Holocene and Pleistocene, they differ in that Barnes was covered by the Laurentide ice sheet while

Agassiz was not. Consequently this placed Barnes in a higher and colder setting than Agassiz in the pre-Holocene epoch. The preferential fractionation of heavy isotopes in warmer conditions would tend to promote enrichment in Agassiz. Also, due to storage conditions, it is suggested that lighter isotopes would diffuse faster, resulting in enrichment in Agassiz. As predicted, values of A93.2 are more enriched than B-White.

5 Results - Aufeis ice and ground ice

Aufeis ice, unlike glacier ice, represents a gas entrapment process which is largely or entirely a consequence of air dissolution in water followed by exsolution during freezing. Ground ice is similarly a consequence of gas dissolution from groundwater during freezing. Gas bubbles found in ground ice are similarly a consequence of gas dissolution from groundwater during freezing. Results of the aufeis ice and ground ice are presented in Table 8.

The concentration of O_2 (in ppm) was obtained using a simple calculation. First it is assumed that the quantity of argon dissolved into the water is equal to its solubility at standard pressure and temperature of 0°C. This assumption is plausible because argon is an inert gas and has continuous supply available. We know that at 0°C, the dissolution for argon is 5E-4 cc_{gas}/cc_{water} and that the mole fraction of argon in air is 0.00934. The mass spectrometer measures O_2/Ar and by multiplying this value by the solubility of argon (5E-4) we obtain the value in cc_{gas}/cc_{water} for O_2. It is then simply a matter of converting the value to ppm.

Table 8 Molar ratio and isotope data for exsolved gases in aufeis ice and ground ice

Sample	$\delta^{18}O$ (‰)	$\delta^{15}N$ (‰)	O_2/Ar (molar)	N_2/Ar (molar)	O_2/N_2 (molar)	O_2 (ppm)
		Firth River 4				
1	-0.7513	-0.4615	18.3127	70.4149	0.2578	13.0642
		Firth River 2				
1	-3.9329	-0.6199	14.3598	61.8790	0.2300	10.2442
2	-3.0626	-0.3323	14.5503	61.4942	0.2345	10.3802
3	-3.9822	-0.7288	15.8267	72.0352	0.2178	11.2907
4	-2.2034	0.0232	17.2320	58.4140	0.2924	12.2932
Average	-3.2953	-0.4145	15.4922	63.4556	0.2437	11.0521
Standard deviation	0.8416	0.3363	1.3302	5.9262	0.0332	0.9490
		Firth River 3				
20.5 - 26	-1.7263	0.3628	17.2214	63.0741	0.2706	12.2857
23/24	-1.5937	-0.8327	17.6451	85.6206	0.2043	12.5879
28/29 - 1	-1.3804	0.0987	17.2319	56.8042	0.3007	12.2932
28/29 - 2	-0.9676	0.1297	16.6360	56.7593	0.2905	11.8681
30/31	-0.5230	0.1367	19.9633	60.6799	0.3261	14.2417
31.0 - 45.5	-0.6665	0.5388	18.8361	70.0480	0.2665	13.4376
31 - 45.5	-0.6097	0.9209	17.8755	60.4163	0.2932	12.7523
36/37 - 1	-1.5175	-0.5033	20.3191	60.2636	0.3342	14.4956
36/37 - 2	-1.4047	-0.6933	20.5707	69.5640	0.2931	14.6750
42/44	0.0433	0.1307	20.1197	73.2109	0.2724	14.3533
9/10 4 - 62 50 - 70	-1.3794	0.2487	18.2851	77.9312	0.2325	13.0445
0 - 10 84	-0.1900	0.1217	20.7288	87.0635	0.2360	14.7879
Average	-0.9930	0.0549	18.7860	68.4530	0.2767	13.4019
Standard deviation	0.5906	0.5045	1.4877	10.6633	0.0382	1.0613
		BSO				
301	0.5358	0.2697	1.3440	62.2114	0.0214	0.9588
		BGR				
254 - 288(1)	2.4530	0.4338	2.8754	58.3071	0.0489	2.0513
288(2) - 1.46	2.9346	0.4068	3.1187	54.7919	0.0564	2.2249
Average	2.6938	0.4203	2.9970	56.5495	0.0526	2.1381
Standard deviation	0.3405	0.0191	0.1721	2.4857	0.0053	0.1227

5.1 Description of the results of aufeis ice and ground ice

On average, the N_2/Ar and O_2/Ar ratios in the aufeis ice from Firth River were found to be lower in the samples from FR2 location compared with FR4 and FR3. The averages of those ratios for FR2 are 15.5 and 63.5, respectively for FR2. The O_2/N_2 ratio is constant throughout the Firth River samples with an average value of 0.27 and a standard deviation of 0.04. The

concentration of oxygen for the Firth River samples is relatively constant and has an average value of 13 ppm.

The O_2/Ar ratios in the gas sampled from ground ice in Nunavik are lower than in the Firth River samples. The average value of samples from both the BSO and BGR location was approximately 2.4 in the ground ice as opposed to 18 in the aufeis ice. The values of N_2/Ar ratios in the gases from the ground ice are closer to those of the aufeis ice compared with the O_2/Ar. The ground ice values of the O_2/N_2 ratio are similar to air while the concentration of oxygen was low with an average value of 1.7 ppm.

Each sampling site for both the ground ice and the aufeis ice samples has unique oxygen isotopic values. While the ground ice values are enriched in oxygen-18, all samples of aufeis ice were depleted with the exception of on sample from FR3. The most depleted samples in the Firth River are found in FR2 while FR3 has the less depleted for this sampling site. The average $\delta^{18}O$ values for FR2 and FR3 are–3.3 ‰ and –0.99 ‰, respectively.

Values of $\delta^{15}N$ were found to be similar to zero (atmospheric) for the aufeis ice samples of the Firth River. On the other hand, the $\delta^{15}N$ values for the ground ice samples appear.

5.2 Synthesis - aufeis ice and ground ice

A distinction between aufeis ice, ground ice and atmospheric values can be made by comparing their O_2/Ar and N_2/Ar ratios. Figure 24 shows that the ground ice has lower O_2/Ar ratios than the dissolved gas content in fresh water at STP, the aufeis ice and atmospheric values are also lower than both the dissolved theoretical content in freshwater at STP and

atmospheric values, although not as low as the ground ice. The N_2/Ar ratios are similar to the dissolved content when some excess air is present.

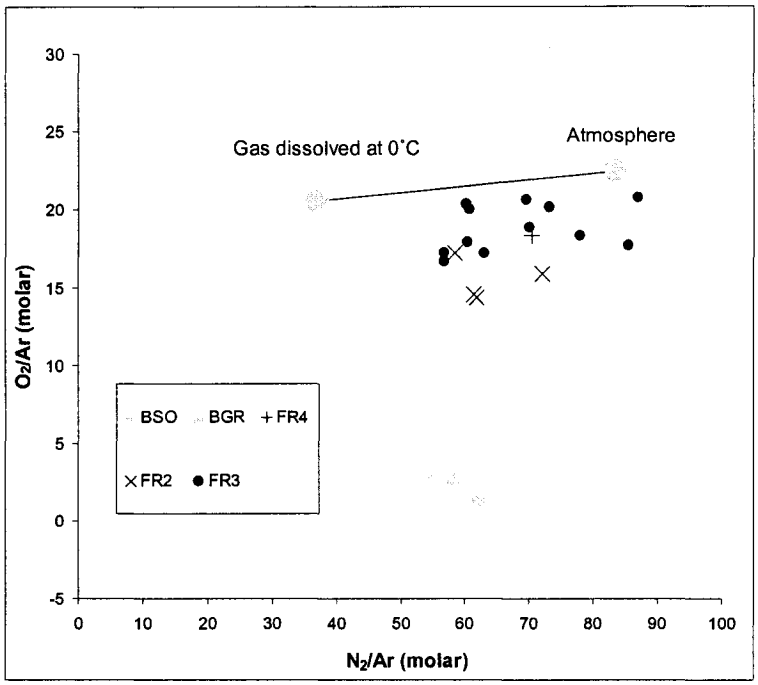

Figure 24 Gas ratios of aufeis ice and ground ice compared with freshwater at STP (0°C, 1 atm) and atmospheric values

Since argon is an inert gas and is continuously available, it can be assumed that a change in ratio is a result of a shortage in the O_2 supply in the ground ice. The hypothesis that the water found in the ground ice mounds was a remnant of the Tyrell Sea was rejected because of negligible salinity of the pore water (Calmels and Allard, 2004). Consequently, it is suggested to have been supplied through groundwater. In this case, the ground ice formed in a location where *in situ* respiration consumed the majority of the available O_2 to negligible levels. This process accounts for the observed O_2/Ar ratio depletion below.

On the other hand, the values of the N_2/Ar ratio are higher than the expected value of gases in freshwater at atmospheric equilibrium. There are 2 possible processes that can explain this

difference: denitrification or the addition of excess air. As the setting is an anoxic environment, denitrification can occur, producing extra N_2. This presumes that a source of NO_3^- was available in the groundwater. Alternatively, addition of excess air in the groundwater is also a valid possibility as fine sediments, such as the silts found in this area, can provide favorable conditions for this process (Heaton and Vogel, 1981). Addition of excess air would move values further from freshwater equilibrium. The N_2/Ar ratios fall within a range of dissolved gas in freshwater at STP with approximately 0.05 cc/cc in excess air content. There is no indication that either scenario is more prevalent making it also possible that the observed ratios are a result of a combination of these two processes.

In the aufeis ice, the N_2/Ar ratios are also higher than the values for freshwater atmospheric equilibrium at STP. Groundwater, which partly supplies water to the aufeis ice, may be subject to higher pressure conditions, which would promote the presence of excess air. If the only process affecting the gas ratio is excess air, then based on Figure 4, the average N_2/Ar ratio corresponds to freshwater equilibrium values with an excess air component of approximately 0.08 cc/cc. There is also a possibility that the N_2/Ar molar ratio reflects groundwater mixing with air from snowpack that may have accumulated on the ice before groundwater discharge onto the surface. In this scenario, the gas content would be composed of the dissolved content in the groundwater with an atmospheric signal originating from air in the snow.

The O_2/Ar ratios of the aufeis ice are lower than the dissolved content from freshwater equilibrium. Once again, argon is non-reactive and would remain unchanged during the residence time of the groundwater examined. Therefore the low O_2/Ar ratios are likely a result of a loss of oxygen. Previous work done in the area by Clark and Lauriol (1997)

indicated that there was production of biogenic methane in these groundwaters (i.e. methanogenese). This process requires the absence of O_2. The gas ratios measured in gas bubbles trapped in aufeis ice show that there was in fact some O_2 which is therefore likely attributable to mixing with air in snow.

The values of $\delta^{18}O$ for FR4, FR2, FR3 and BSO-BGR are distinct from one another (Figure 25). The gas found in ground ice is enriched in oxygen-18, especially in BGR while aufeis ice is depleted in oxygen-18.

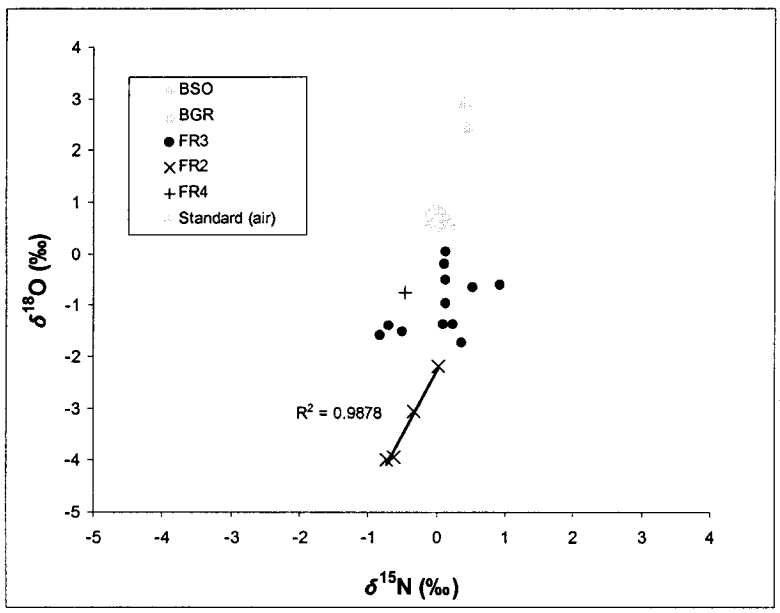

Figure 25 Isotopic content of oxygen-18 and nitrogen-15 in ground ice and aufeis ice

The isotopic values of oxygen-18 in the Firth River aufeis ice samples are heterogeneous, ranging from a depleted value of -3.98 ‰ to an enriched value of +0.04 ‰. The isotopic content dissolved in freshwater at STP would tend to be enriched by +0.7 ‰ (Benson and Krause, 1984), but is found to be mostly depleted in Firth River. As mentioned earlier, it is likely that this is a result of groundwater mixing with snow accumulated on top of the aufeis

ice before freezing. This conclusion is also supported by the relatively higher concentration of O_2 present in the aufeis ice as shown in Figure 26. This figure indicates a positive trend between O_2 concentration and oxygen-18 signature, reflecting the mixing.

As mentioned, low O_2/Ar ratios in the ground ice suggest that respiration had an effect on the oxygen composition of the dissolved gases. During respiration, there is a preferential consumption of the lighter oxygen isotopes, creating an enriched isotopic ratio (Schleser, 1979; Quay and al., 1995). The enriched $\delta^{18}O$ signature observed in BSR and BGR is likely a result of this process. In addition, the effect of respiration on O_2 concentration is evidenced in Figure 26.

The values of $\delta^{15}N$ are close to zero for both types of ice. BSO and BGR are slightly enriched in nitrogen-15 while FR2 and FR4 are depleted. The average $\delta^{15}N$ of the ground ice is enriched in comparison with atmospheric values. During denitrification, preferential consumption of lighter isotopes of nitrogen results in an enriched $\delta^{15}N$ signature in nitrate (Llund et *al.*, 2000). However, because precision of $\delta^{15}N$ is ±0.54, it cannot be determined if the observed enrichment is indeed a result of denitrification, excess air or a combination of both. The average $\delta^{15}N$ in the gas trapped in the Firth River ice samples is -0.015 ‰ suggesting these processes were absent here.

A comparison of the $\delta^{18}O$ and the O_2 concentration (Figure 26) reveals a positive trend in the aufeis ice data with a correlation coefficient of 83.41%. Generally, lower concentrations of O_2 are associated with FR2. There are not enough points to discern a trend in the ground ice.

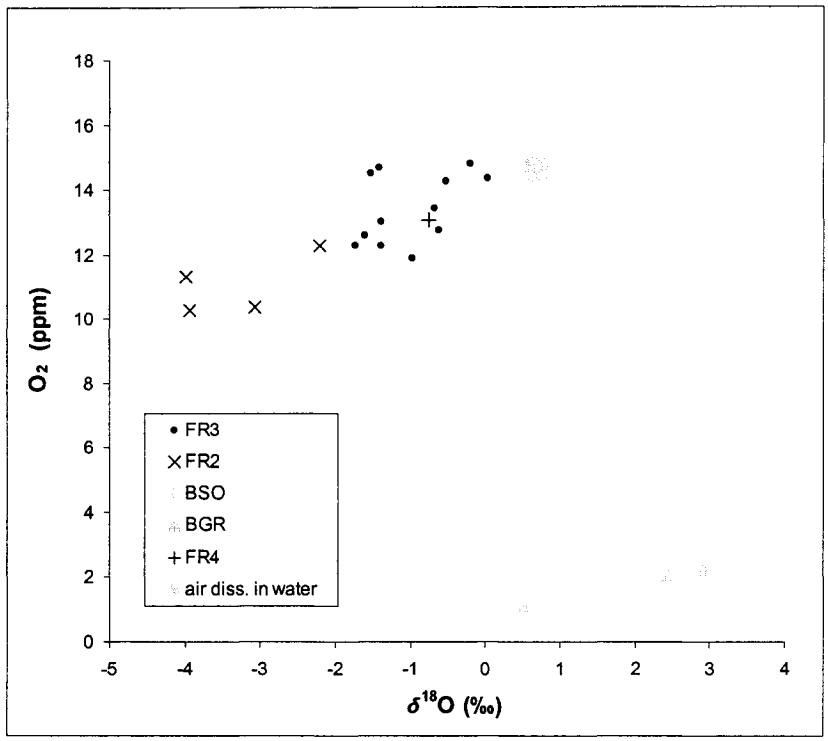

Figure 26 Comparison of O_2 concentration and oxygen isotopic content in aufeis ice and ground ice

6 Comparison of all sites

Comparison of all three types of ice indicates that each type has a distinct gas signature as shown in Figure 27 and Figure 28. The gases trapped in ground ice have considerably lower O_2/Ar ratios than those found in glacier ice, aufeis ice, the atmosphere and in gas dissolved in freshwater at STP. Glaciers generally have a higher O_2/Ar ratio than aufeis ice and ground ice because their gas content is essentially an atmospheric signal as shown in Figure 27. Similarly, the N_2/Ar ratio in Barnes and Agassiz are close to the atmospheric ratio.

On the other hand, aufeis ice has lower O_2/Ar ratios than glacier ice because their content reflects the freshwater solubility of gases. Similarly, N_2/Ar ratios in aufeis ice are lower than those of glacier ice and atmosphere.

Ground ice sampled in this study has low O_2/Ar ratios than both glacier and aufeis ice because of the effect of respiration. On the other hand, its N_2/Ar is higher than the theoretical value of dissolved gas, reflecting processes of denitrification and/or excess air incorporated during recharge.

A comparison of the $\delta^{15}N$ and $\delta^{18}O$ (Figure 28) suggests that although there is some crossing of values, most sites have a unique signature, particularly a unique $\delta^{18}O$ signature. An analysis of variance shows that there is a highly significant difference between the different sampling sites for both $\delta^{15}N$ and $\delta^{18}O$.

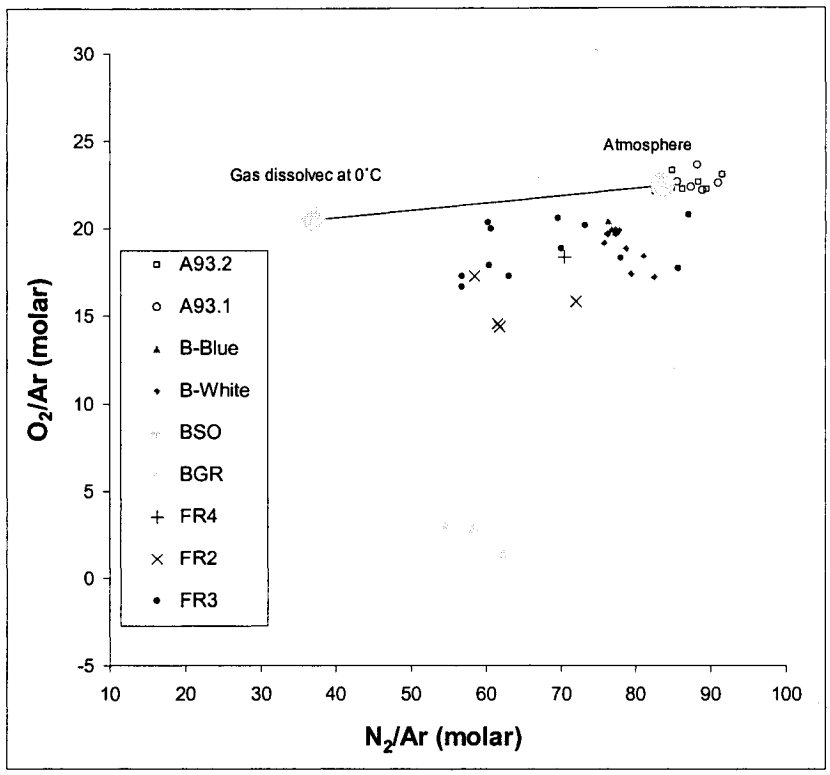

Figure 27 Comparison of molar gas ratios (O_2/Ar and N_2/Ar) of all sampled sites with atmospheric values and gases dissolved in freshwater at 0°C.

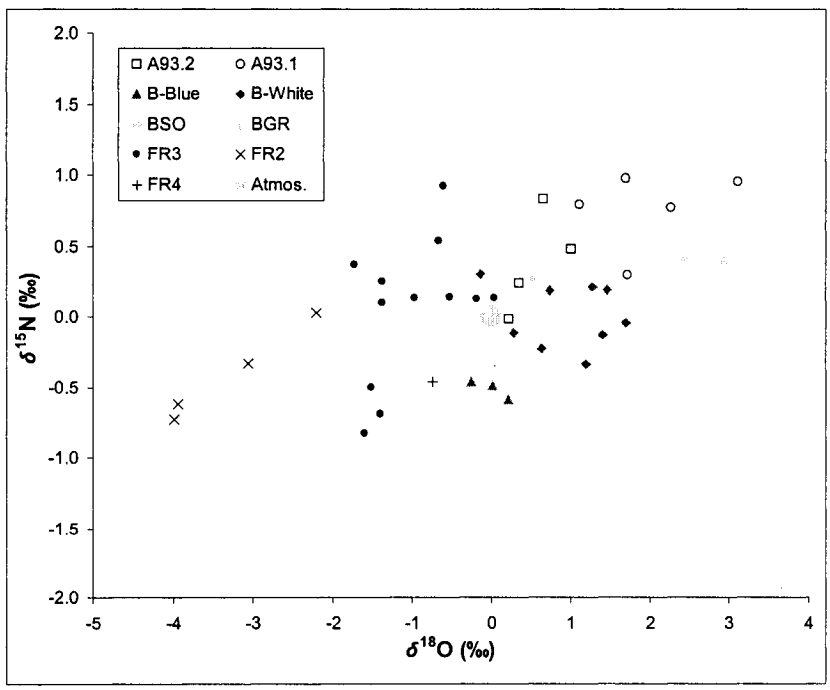

Figure 28 Comparison of oxygen-18 and nitrogen-15 content in every sampling site

A scattering of all data points around the atmospheric value can be observed when comparing O_2/Ar with $\delta^{18}O$ (Figure 29). There is a generally positive trend for all types of ice in that as $\delta^{18}O$ increases, so does O_2/Ar. This comparison also suggests a difference in the types of samples which is supported by an analysis of variance. Results of the analysis of variance show that there is a highly significant difference between the values of O_2/Ar for all sampling sites. Glacier samples from Agassiz and Barnes and ground ice samples (BGR and BSO) have fall to the right of the atmospheric value indicating an enriched isotopic values for oxygen-18. On the other hand the aufeis ice from Firth River has a depleted $\delta^{18}O$ signal compared to all other points.

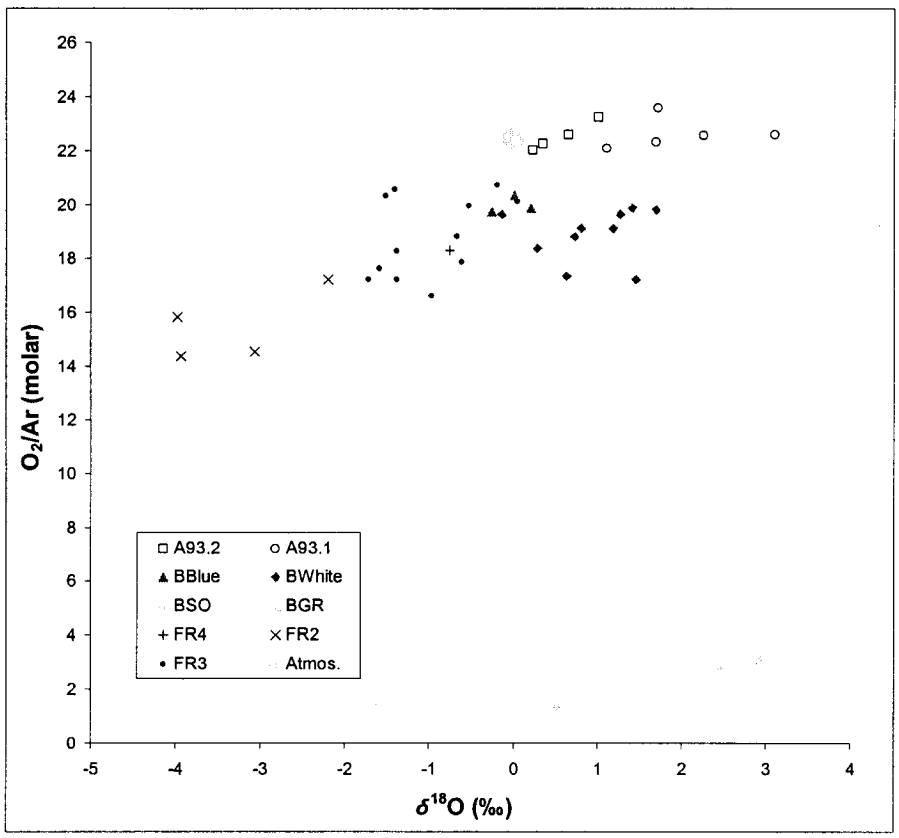

Figure 29 Oxygen and Argon ratio and oxygen isotopic content in every sampling site

The comparison above provides a clear indication that each type of ice has a distinct gas signature. The following summarizes ranges and values provided in earlier sections. Generally, the isotopic content trapped in glacier ice cores ranges between –0.3 and 2.3 ‰ and between –0.6 and 1 ‰ for $\delta^{18}O$ and $\delta^{15}N$, respectively. The molar ratios O_2/Ar (22.4) and N_2/Ar (83.6) in the atmosphere are similar to those found in atmosphere trapped in glacier ice core. The O_2/Ar in Agassiz and Barnes ice cores varies between 17.4 and 23.6 while the N_2/Ar varies between 75.8 and 91.5. Gas trapped in buried ice would be expected to fall within those ranges.

Isotopic values of the aufeis ice at Firth River range between –4.0 and 0.0 ‰ and between –0.8 and 0.9 ‰ for $\delta^{18}O$ and $\delta^{15}N$, respectively. The molar ratio O_2/Ar varies between 56.8 and 87.1, while N_2/Ar varies between 14.4 and 20.7. The isotopic content of gases trapped in ground ice resulting from ice segregation varies between 0.5 and 3.0 ‰ for $\delta^{18}O$ and between 0.4 and 0.4 ‰ for $\delta^{15}N$. The molar ratios range between 1.3 and 3.1 for O_2/Ar and between 54.8 and 62.2 for N_2/Ar. Isotopic values and molar ratios measured in gas bubbles from ice falling in the ranges described above can be used to delineate between glacier, aufeis or segregated ice origin.

7 Conclusion

An extraction line that uses liquid helium to isolate atmospheric gases trapped in ice was constructed based on a design by Sowers and Bender (1989). A new method for rapid analysis of gas molar ratios and isotope ratios was developed, based on dilution in helium gas coupled with analysis using a continuous flow isotope ratio mass spectrometry. A series of leak tests, calibration, background checks and reproducibility tests were performed to ensure the precision and stability of the extraction method. The precision of the measurements resulting from the method, based on the use of standard air introduced into the extraction line are ±18.2 for N_2/Ar, ±1.3 for O_2/Ar, ±0.7 for $\delta^{18}O$ of O_2 and ±0.5 for $\delta^{15}N$ of N_2. Once the extraction line and mass spectrometry were established, an air standard followed by samples analysis was completed. Samples of different ice types were selected, including glacier ice from the Agassiz ice cap and the Barnes ice cap, aufeis ice from Firth River and ground ice from Nunavik.

Agassiz ice showed enriched values for $\delta^{15}N$ of N_2 and $\delta^{18}O$ of O_2 compared to present day atmosphere. The $\delta^{18}O$ varies between 0.3 ‰ and 3.1 ‰ while the $\delta^{15}N$ varies between 0 ‰ and 1 ‰. O_2/Ar and N_2/Ar gas ratios are higher than any other type of ice analyzed during this research and higher than atmospheric ratios, with average values of 22.5 and 87.0, respectively. Those values may have been affected by microfractures which led to preferential argon loss. The higher $\delta^{18}O$ are associated with a colder environment (i.e. pre-Holocene). The pre-Holocene period would be represented by samples of core A93.1, taken deeper than approximately 109m.

The O_2/Ar and N_2/Ar ratios of Barnes ice cap were found to be slightly lower than theoretical atmospheric ratios. This was expected because of gravitational settling and confirms the

efficiency of the extraction and analysis method. The samples analyzed were taken from ice dated as pre-Holocene and Holocene (Zdanowicz et *al.*, 2002). The isotopic ratios were found to be less enriched than the ones of Agassiz. Isotopic ratios $\delta^{18}O$ of O_2 of B-White ice formed during pre-Holocene were higher than present day atmospheric ratios with an enriched average value of 0.5 ‰. Gravitational settling is responsible for the higher gas and isotopic ratios. This effect is intensified in a colder environment. During the last glaciation, Barnes was part of the Laurentide ice sheet, with accumulation at much higher altitude and colder temperature than today. Samples of B-Blue are more representative of present day gas ratios and isotopic content. B-Blue was most likely accumulated during the change from pre-Holocene to Holocene.

Despite the low number of ground-ice samples available for this study, the results provided information relevant to the origin of the groundwater and geochemical conditions in the area prior to permafrost aggradation. Gas ratios as well as O_2 ppm concentrations revealed that there is very little oxygen in the gas trapped in the ground ice analyzed suggesting it was previously consumed through respiration. The dissolved concentration of O_2 in the ground ice samples averages at 1.7 ppm. This is well below the theoretical value of 14.6 ppm in freshwater at equilibrium with atmosphere. The enriched $\delta^{18}O$ also suggests consumption of O_2 through respiration, a process during which there is a preferential consumption of the lighter isotopes (Schleser, 1979; Quay and al., 1995). On the other hand, results of N_2/Ar are higher than the theoretical dissolved ratio. Because it is assumed that argon is always available, it is concluded that there is an input of N_2 either from the process of denitrification, which takes place in oxygen-free environments, or from the addition of excess air, or a combination of both. The average $\delta^{15}N$ is 0.4 ‰, which is only slightly higher than average value of the standard air.

Aufeis ice display heterogeneous values for both gas ratios and isotopic content. The molar O_2/Ar values range from 14.4 to 20.7. The theoretical molar ratio of gases dissolved in equilibrium with atmosphere is 20.5 while the ratio in atmosphere 22.4. Although methanogenesis has been identified as a potential process in the groundwater discharge in this region (Clark and Lauriol, 1997), which requires the absence of O_2, the heterogeneity of the values suggests that there is a presence of O_2 in the water. The input of oxygen to the water was likely a result of mixing of groundwater source with air from snow on the surface of the aufeis ice, before freezing. The ratios would then represent a mixture of dissolved gas in the groundwater and an atmospheric signal from the snow. The N_2/Ar molar ratio are all greater than the ratios of dissolved gas at freshwater equilibrium with atmosphere suggesting a mixture of excess air and dissolved gases in the groundwater with snow. The aufeis ice is depleted in ^{18}O of O_2 and its isotopic content of ^{15}N of N_2 is approximately -0.1 ‰.

All sites analyzed displayed different gas ratios and isotopic content. The glaciers Agassiz and Barnes generally hold the highest molar ratios of O_2/Ar and N_2/Ar, while the ground ice samples display the lowest. This is a direct consequence of the entrapment of air directly from the atmosphere versus the dissolution of gases in water. Aufeis ice is somewhat in the middle with heterogeneous values that reflect the incorporation of dissolved gases and the direct incorporation of air through saturation and freezing of snow on the aufeis surface. The $\delta^{18}O$ of O_2 found in glacier ice and ground ice was found to be generally enriched with respect to present day air while it is depleted in the aufeis ice. The $\delta^{15}N$ of N_2 is enriched in Agassiz and in the ground ice but averages at approximately 0 ‰ in Barnes ice and aufeis ice of the Firth River.

This research examines, for the first time, the use of molar gas ratios and isotope ratios obtained from gas bubbles entrapped in ice. Further analysis should be completed with this technique to understand more about the origin of formation of ice types. Ideally, gas ratios and isotopic ratios of gas trapped in ice combined with other analysis should provide a better understanding of processes involved in the environment where the ice is found. An improvement of the analytical precision and more samples with better field control would allow better identification of the signature for different types of ice.

References

Allard M, Seguin MK, Levesque R. 1987. The Holocene evolution of permafrost near the tree line, on the eastern coast of Hudson bay (Northern Quebec). *Canadian journal of Earth Sciences* **24**: p. 2006-2222.

Andrews, J.N., 1992. Mechanisms for noble gas dissolution by groundwater. *Isotopes of Noble Gases as Tracers in Environmental Studies*. International Atomic Energy Agency, Vienna, p. 87-109.

Barnola, J.M., Pimienta, P., Raynaud, D., Korotkevich, Y.S., 1991. CO_2 climate relationship as deduced from the Vostok ice core: A reexamination based on new measurements and on reevaluation of the air dating, *Tellus*, 43 (B), p. 83-90.

Bender, M.L., Labeyrie, L., Raynaud, D., Lorius, C., 1985. Isotopic composition of atmospheric O_2 linked with deglaciation and global primary productivity. *Nature*, 318, p. 349-352.

Bender, M., Sowers, T., Dickson, M., Orchardo, J., Grootes, P., Mayewski, P.A., Meese, D.A., 1994. Climate correlations between Greenland and Antarctica during the past 1000,000 years. *Nature*, vol 372, p. 663-666.

Benson, B.B., Krause, D.Jr., 1980. The concentration and Isotopic fractionation of gases dissolved in freshwater in equilibrium with the atmosphere. 1. Oxygen. *Limnology and Oceanography*, Vol 25, No. 4, p. 662-671.

Benson, B.B., Krause, D.Jr., 1984. The concentration and Isotopic franctionation of oxygen dissolved in freshwater and seawater in equilibrium with the atmosphere. *Limnology and Oceanography*, Vol 29, No. 3, p. 662-632.

Brouchkov, A., Fukuda, M., 2002. Preliminary measurements on methane content in permafrost, Central Yakutia, and some experimental data. *Permafrost and periglacial processes*, 13, p. 187-197.

Caillon, N., Severinghaus, J.P., Jouzel,J., Barnola, J., Kang, J., Lipenkov, V.Y., 2003. Timing of Atmospheric CO_2 and Antarctic Temperature Changes across Termination III. *Science*, vol 299, p. 1728-1731.

Calmels, F., Allard, M., 2004. Ice segregation and gas distribution in permafrost using tomodensitometric analysis. *Permafrost and periglacial processes*, 15, p. 367-378.

Castelnau, O., Duval, P. 1994. Simulations of anisotrophy and fabric development in polar ices. *Annals of glaciology*, 20, p. 277-282.

Chappellaz, J., Barnola, J.-M., Raynaud, D., Korotkevich, Y.S., Lorius, C., 1990. Ice-core record of atmospheric methane over the past 160,000 years, *Nature*, 345, p.127-131.

Clark, I.D., Fritz, P., 1997, Environmental isotopes in hydrogeology, Lewis publishers, Boca Raton, FL, 328p.

Clark, I.D. and Lauriol, B., 1997. Aufeis of the Firth River Basin, Northern Yukon, Canada: Insights into Permafrost Hydrogeology and Karst. *Arctic and Alpine Research*, Vol 29, No. 2, p. 240-252.

Craig, H., Horibe, Y., Sower, T. 1988. Gravitational Separation of gases and isotopes in polar ice caps. *Science*, vol 242, p. 1675-1678.

CRC handbook of chemistry and physics, Editor: Robert C. Weast, published by: The chemical rubber Co., Boca Raton, Florida, 1988.

Dallimore, S.A., Wolfe, S.A., 1988. Massive ground ice associated with glaciofluvial sediments, Richards Islands, N.W.T., Canada. In: *Permafrost, Fifth International Conference*, Proceedings, vol. 1. Tapir, Trondheim, p. 132-137.

Dansgaard, W., Stable isotopes in precipitation, *Tellus*, 16, p. 436-468, 1964.

Dongmann, G., 1974. The contribution of land photosynthesis to the stationary enrichment of ^{18}O in the atmosphere, *Radiat. Environ, Biophys.*, 11, p. 219-225.

Dredge, L.A., Kerr, D.E., Wolfe, S.A., 1999. Surficial materials and related ground ice conditions, Slave Province, N.W.T., Canada, *Canadian Journal of Earth Sciences*, 36, p. 1227-1238.

Dyke, A.S., Prest, V.K., 1987. Late Wisconsinian and Holocene history of the Laurentide Ice-sheet, *Géographie Physique et Quaternaire*, 41, p. 237-263.

Dyke, A.S., Savelle, J.M., 2000. Major end moraines of Younger Dryas age on Wollaston Peninsula, Victoria Island, Canadian Arctic : implications for paleoclimate and for formation of hummocky moraine, *Canadian Journal of Earth Sciences*, 37, p. 601-619.

Fisher, D.A., Koerner, R.M., Paterson, W.S.B., Dansgaard, W., Gundestrup, N., Reeh, N., 1983. Effect of wind scouring on climatic records from ice-core oxygen-isotope profiles. *Nature*, vol **301**, 20, p. 205-209.

Ford, D.C., 1996. Karst in a cold climate: Effects of glaciation and permafrost conditions upon the karst landforms systems of Canada. In: *McCann, B.Sc., Ford, D.C. (Eds.), geomorphology Sans Frontières.* Wiley, New York, p. 153-179.

French, H.M., Harry, D.G., 1990. Observations on buried glacier ice and massive segregated ice, western Arctic coast, Canada. *Permafrost and Periglacial Processes* 1, p. 31-43.

French, H.M., 1996, The periglacial environment, Second edition, Longman, England, 341p.

Fujino, K., Sato, S., Matsuda, K., Sada, G., Shimizu, O., Kato, K., 1998. Characteristics of the massive ground ice body in the western Canadian Arctic. *Proceedings of the Fifth International Conference on Permafrost,* Trondheim, Norway, August 1988, p. 143-147.

Guglielmin, M., Camusso, M., Polesello, S., Valsecchi, S., Teruzzi, M., 2002. A note on the Ice Crystallography and Geochemistry of a Debris Cone, Northern Foothills, Antarctica. *Permafrost and periglacial processes*, 13, p. 77-82.

Handbook of chemistry and physics, Editor: Robert C. Weast, published by: The chemical rubber Co., Cleveland, Ohio, 1970.

Harry, D.G., French, H.M., Pollard, W.H., 1988. Massive ground ice and ice-cored terrain near Sabine Point, Yukon Coastal Plain. *Canadian journal of Earth Sciences 25*, p. 1846-1856.

Hattori, A., 1983. Denitrification and dissimilatory nitrate reduction, *Nitrogen in the marine environment*, edited by E.J. Carpenter and D.G. Capone, p. 191-141, Academic Press, San Diego, Calif.

Heaton, T.H.E., Vogel, J.C., 1981, "Excess air" in groundwater. *Journal of Hydrology*, 50. p. 201-216.

Hu, X., Pollard, W.H., 1997. Ground Icing Formation: Experimental and Statistical Analyses of the Overflow Process. *Permafrost and Periglacial Processes*, Vol 8, p. 217-235.

Killawee, J.A., Fairchild, I.J., Tison, J.-L., Janssens, L., Lorrain, R., 1998. Segregation of solutes and gases in experimental freezing of dilute solutions: Implications for natural glacial systems. *Geochimica et Cosmochimica Acta*, Vol 62, No 23/24, p. 3637-3655.

Koerner, R.M., Fisher, D.A., 1990. A record of Holocene summer climate from a Canadian high-Arctic ice core. *Nature*, vol. 343, No. 6259, p. 630-631.

Kroopnick, P., Craig, H., 1972. Atmospheric oxygen: Isotopic composition and solubility fractionation, *Science*, 175, p. 54-55.

Lacelle, D., Bkornson, J., Lauriol, B., Clark, I.D., Troutet, Y., 2004. Segregated-intrusive ice of subglacial meltwater origin in retrogressive thaw flow headwalls, Richardson Mountains, NWT, Canada. *Quaternary Science Reviews* 23, p. 681-696.

Lajeunesse, P., Allard, M., 2003. The Nastapoka drift belt, eastern Hudson Bay: implication of s astilsand of the Quebec-Labrador ice margin in the Tyrell Sea at 8 Ka BP. *Canadian Journal of Earth Sciences* **40**: p. 65-76.

Llund, L.J., Horne, A.J., Williams, A.E., 2000. Estimating denitrification in a large constructed wetland using stable nitrogen isotope ratios. *Ecological engineering*, 14, p. 68-76.

Lorrain, R.D., Demeur, P., 1985. isotopic evidence for relic Pleistocene glacier ice on Victoria Island, Canadian Arctic Archipelago. *Arctic and Alpine Research 17*, p. 89-98.

MacKay, J.R., 1966. Segregated epigenetic ice and slumps in permafrost, Mackenzie Delta area, N.W.T. *Geographical Bulletin 8*, p. 59-80.

MacKay, J.R., 1971. The origin of massive icy beds in permafrost, western Arctic coast, Canada. *Canadian journal of Earth sciences*, 8, p. 397-422.

MacKay, J.R., Dallimore, S.R., 1992. Massive ice of the Tuktoyaktuk area, western Arctic coast, Canada. *Canadian Journal of Earth Sciences 29,* p. 1235-1249.

Maupetit, F., Wagenbach, D., Weddeling, P., Delmas, R.J., 1995. Seasonal fluxes of major ions to a high altitude cold alpine glacier. *Atmospheric environment,* vol 29, No 1, p. 1-9.

Mariotti, A., 1983. Atmospheric nitrogen is a reliable standard for natural 15N abundance measurements, *Nature*, 303, p. 685-687.

Moorman, B.J., Michel, F.A., Wilson, A., 1996. ^{14}C dating of trapped gases in massive ground ice, Western Canadian Arctic. *Permafrost and Periglacial processes*, 7, p. 257-266.

Moorman, B., Michel, F.A., Wilson, A.T., 1998. The development of tabular massive ground ice at Peninsula Point, N.W.T., Canada. In: *Proceedings of the Seventh International Conference on Permafrost, Yellowknife, Canada, 23-27 June 1998.* Collection Nordicana, Centre d'études nordiques. Universit/ Laval, p. 757-762.

Morland, L.W., Staroszcyk, R. 1998. Viscous response of polar ice with evolving fabric. *Continuum mechanism thermodynamics*, 10, p. 135-152.

Murton, J.B., Whiteman, C.A., Waller, R.I., Pollard, W., Clark, I.D., Dallimore, S.R., 2005. Basal ice facies and supraglacial melt-out till of the Laurentide Ice Sheet, Tuktoyaktuk Coastlands, western Arctic Canada, *Quaternary Science Reviews*, 24, p. 681-708.

Neftel, A., Oeschger, H., Staffelbach, T., Stauffer, B., 1988. CO_2 record in the Byrd ice core 50,000-5,000 B.P., *Nature*, 320, p. 248-250.

Pollard, W.H., 1991. Observations on massive ground ice on Fosheim Peninsula, Ellesmere Island, Northwest Territories. Current Research, Part E: Geological Survey of Canada 91-1E, p. 223-231.

Pollard, W.H., Dallimore, S.R., 1988. Petrographic characteristics of massive ground ice, Yukon Coastal Plain, Canada. In: *Permafrost, Fifth International Conference,* Proceedings, vol. 1. Tapir, Trondheim, p. 224-229.

Quay, P.D., Wilbur, D.O., Richey, J.E., Devol, A.H., Benner, R., Forsberg, B.R., 1995. The ^{18}O:^{16}O of dissolved oxygen in rivers and lakes in the Amazon Basin: Determining the ratio of respiration to photosynthesis rates in freshwaters, *Limnol. Oceanogr.*, 40(4), p. 718-729.

Rampton, V.N., 1974. The influence of ground ice and thermokarst upon the geomorphology of the Mackenzie-Beaufort region. In: *Alpine Geomorphology, Proceedings of the Third Guelph Symposium on Geomorphology.* Geo-Abstracts, Norwich, p. 43-59.

Rampton, V.N., 1988. Origin of massive ground ice on Tuktoyaktuk Peninsula, Northwest Territories, Canada: a review of stratigraphic and geomorphic evidence. In: Fifth International Conference, Proceedings, vol. 1. Tapir, Trondheim, p. 850-855.

Schleser, G.H., 1979. Oxygen isotope fractionation during respiration for different temperatures of *T. utilis* and *E. Cole* K12, *Radiat. Environ. Biophys.*, 17, p. 85-93.

Schwander, J., 1996. Gas diffusion in firn. In: Chemical exchange between the atmosphere and polar snow, E.W. Wolfe and R.C. Bales, eds., NATO ASI SERIES, 1 (43), p. 528-540.

Sowers, T., Bender, M. 1989. Elemental and isotopic composition of occluded O_2 and N_2 in polar ice. *Journal of geophysical research*, vol 94, no. D4: p. 5137-5150.

Sowers, T, Bender, M., 1992. $\delta^{15}N$ of N_2 in air trapped in polar ice: a tracer of gas transport in the firn and a possible constraint on ice-age gas differences. Journal of geophysical research, vol 97, no. d14, p. 15,683-15,697.

Sowers, T., Bender, M., Raynaud, D., Korotkevich, Y.S., Orchardo, J., 1991. The $\delta^{18}O$ of atmospheric O_2 from air inclusions in the Vostok ice core: Timing of CO_2 and ice volume changes during the penultimate deglaciation, *aleoceanography*, 6, p. 679-696.

Sowers, T., Brook, E., Etheridge, D., Blunier, T., Fuchs, A., Leuenberger, M., Chappellaz, J., Barnola, J.M., Wahlen, M., Deck, B., and Weyhenmeyer, C., 1997. An interlaboratory comparison of techniques for extracting and analyzing trapped gases in ice cores. *Journal of Geophysical Research*, Vol 102, No C12, p. 26,527-26,538.

St-Onge, D.A., McMartin, I., 1995. The Bluenose Lake Moraine, a moraine with a glacier core, *Géographie Physique et Quaternaire*, 53, p. 287-295.

Williams, P.J., Smith, M.W. 1989. The Frozen Earth, Cambridge University Press, Cambridge, 306p.

Wilson, G.B., McNeill, G.W. 1997. Noble gas recharge temperatures and the excess air component. *Applied Geochemistry*, vol 12, p. 747-762.

Zdanowicz, C.M., Fisher, D.A., Clark, I., Lacelle, D., 2002. An ice-marginal $\delta^{18}O$ record from Barnes Ice Cap, Baffin Island, Canada. Annals of Glaciology 35, p. 145-149.

Zheng, J., Kudo, A., Fisher, D.A., Blake, E.W., Gerasimoff, M., 1998. Solid electrical conductivity (ECM) from four Agassiz ice cores, Ellesmere Island NWT, Canada: high-resolution signal and noise over the last millennium and low resolution over the Holocene. *The Holocene*, **8**, 4: p. 413-421.

Appendix

Mass spectrometer preparation :

1. Attach the proper reference gas to the mass spectrometer (Ref 1 = N_2, Ref 2 = Ar, Ref 3 = O_2)
2. Open the valve for the 3 gases to allow them to flow through MS and to flush air that might have entered the MS for approximately 5 minutes
3. If needed, switch line to proper column (see back of mass spectrometer)
4. Close valves for the 3 gases
5. Adjust the flow of each reference gas so that the voltage is 4,000mV for Ref 1, 19,000 mV for Ref 2 and 7,000 mV for Ref 3.
6. Perform a peak recalibrate
7. Run a bypass (exetainer with air from the lab) to "warm up" the mass spectrometer

Transfer line preparation

1. Flush an exetainer with Helium
2. Run the exetainer on the mass spectrometer to ensure no contamination is induced from the transfer line (values should be extremely low, if not, there is a leak and must be fixed before continuing)

Standard air measurement:

1. Perform leak test on the extracting line by closing the valve connecting the diffusion pump to the extraction line. The reading on the piranni gauge should stay low (< $5*10^{-4}$mTorr). Leave the valve closed
2. Attach glass container to the line
3. Close valve connecting stainless steel tube to the extraction line
4. Insert tube in liquid helium dewar
5. Allow an aliquot of the standard to expand in the line for approximately 2 minutes
6. Open the valve to the tube and let aliquot transfer (see pressure gauge reading decrease) for 10 minutes
7. Close valve connecting the tube to the line
8. Remove tube from liquid helium and let it reach room temperature
9. Transfer the gas from the tube to an exetainer using the transfer line
10. Analyse on mass spectrometer
11. Isotopic values should be similar to other standard results. If not, investigate before continuing with an ice sample

Extraction preparation :

1. Rinse the extraction vessel with distilled water
2. Clean the extraction vessel with acetone
3. Dry in the oven (~50°C) for at least one hour
4. Cool the vessel at room temperature for approximately 30 minutes
5. Suspend the vessel in hemispherical dewar containing chilled ethanol for at least 20 minutes (~-20°C)
6. Transfer ice sample into the vessel using metal tweezers without dropping the ice in the vessel.

7. Attach the vessel to the line. If using the copper gasket, ensure that the gasket was not used more than 3 times.
8. At this point, the valve connecting the stainless steel tube to the extraction line should be closed. Open the valve connecting the vessel to the extraction line.
9. Raise the ethanol bath (~-20°C) so that the part of the vessel where the ice ice is completely covered. Pump for 30 minutes and ensure that the bath temperature stays at -20°C
10. Close the valve connecting to the vessel to the line
11. Open the valve connecting the stainless steel tube to the extraction line.
12. Remove the ethanol bath

Extraction:

1. Slowly immerse the vessel in lukewarm water to initiate melting of the ice (2 minutes)
2. Immerse the vessel in warm tap water until the ice is completely melted
3. Chill the ethanol bath to -75°C
4. Raise the lab jack until the bottom of the vessel touches the ethanol bath
5. When ice is frozen all the way to the top, cool the ethanol to -100°C and raise the dewar until the part containing the ice is completely immersed
6. Freeze for at least 15 minutes
7. Close the valve connecting the stainless steel tube to the extraction line
8. Close the valve connecting the diffusion pump to the extraction line
9. Close the valve connecting the gauge to the line
10. Open the valve connecting the vessel to the extraction line and allow gas to expand in the line for 1 minute
11. Insert the stainless steel tube in the liquid helium dewar
12. Open the valve connecting the stainless steel tube to the line
13. Allow 10 minutes for gas to transfer into the tube. At this point the reading of the pressure gauge will decrease as the gas is being transferred
14. Close the valve connecting the tube to the line
15. Close the valve connecting the vessel to the line
16. Remove the ethanol bath
17. Repeat 13-18
18. Open the valve connecting the vessel to the extraction line and allow gas to expand in the line for 1 minute
19. Open the valve connecting the stainless steel tube to the line
20. Allow 10 minutes for gas to transfer into the tube. At this point the reading of the transducer will decrease until it reaches approximately 0 Torr as the gas is being transferred
21. Close the valve connecting the tube to the line
22. Slowly remove the tube from the liquid Helium dewar
23. Open the valve connecting the piranni gauge to the extraction line. Reading should be $< 3*10^{-3}$ mTorr, if not, it is an indication of a leak
24. Allow to cool down to room temperature for at least 40 minutes
25. Meanwhile, close the valve connecting the vessel to the line
26. Remove the ethanol bath and let the ice melt
27. Once the stainless steel tube is at room temperature, transfer the gas content into an exetainer using the transfer line
28. The gas sample is now ready for analysis on the GC-MS